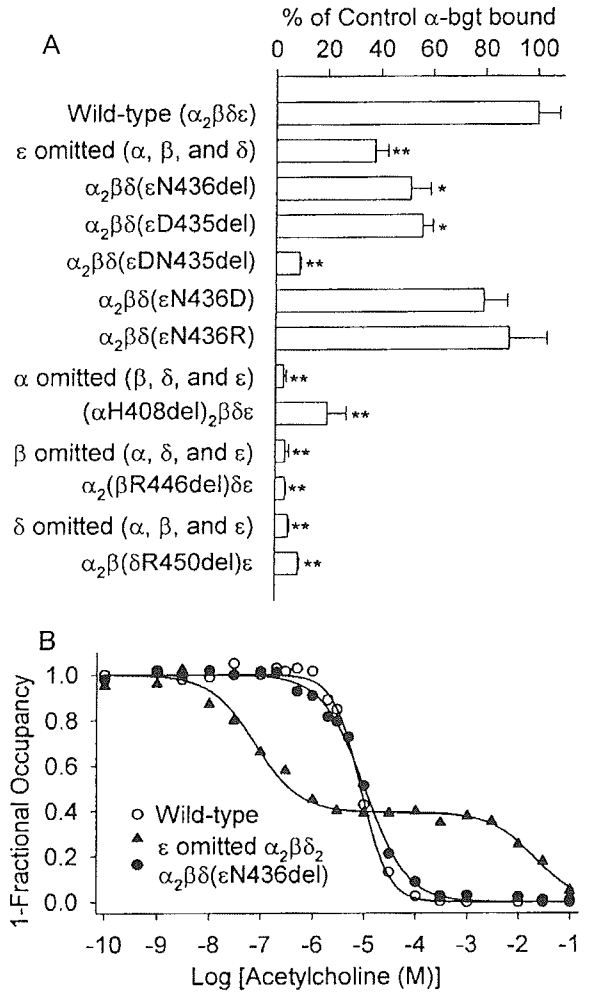

Fig. 4 (**A**) [^{125}I]α-bgt binding to surface receptors on intact HEK cells transfected with the indicated AChR subunits. The results are normalized for α-bgt binding to wild-type AChR and represent the mean and SD of three to six experiments. $^*P < 0.05$; $^{**}P < 0.01$, compared with wild-type AChR. (**B**) ACh binding to intact HEK cells transfected with indicated AChR subunits determined by competition against the initial rate of [^{125}I]α-bgt binding. Curves are fitted to the Hill equation (see Methods). $K_{ov} = 8.69 \times 10^{-6}$, $n = 1.65$ for wild-type AChR; $K_{ov} = 1.03 \times 10^{-5}$, $n = 1.07$ for εN436del-AChR; and $K_A = 7.73 \times 10^{-8}$, $K_B = 2.22 \times 10^{-2}$, $fract_A = 0.61$ for ε-omitted AChR.

the N-terminal end of M4. To determine whether either or both effects reduce expression or alter activation of AChR, we engineered four site-directed mutants (Fig. 3B) and expressed each together with complementary wild-type subunits in HEK cells.

The first engineered mutant, εD435del, shortens the M3–M4 loop by a single residue, without shifting a negative charge against M4 (Fig. 3B). This mutation reduces surface expression of AChR to ~56% of wild-type (Fig. 4A) and decreases the mean durations of the major components of channel openings and bursts (Table 2 and Fig. 5C) to ~65 and ~50% of wild-type, respectively. The second engineered mutant, εDN435del, which removes two residues from the M3–M4 loop (Fig. 3B), reduces AChR expression to ~10% of wild-type, and decreases the mean durations of the longest components of channel openings and bursts to ~65 and ~55% of wild-type, respectively (Table 2 and Fig. 5F). The third and fourth engineered mutants, εN436R and εN436D, do not shorten the M3–M4 loop but position a positive or negative charge next to M4 (Fig. 3B). Neither mutant has an appreciable effect on AChR surface expression (Fig. 4A) or channel kinetics (Table 2 and Fig. 5D and E). Thus, the effects of εN436del on AChR expression and channel kinetics can be attributed to shortening of the M3–M4 loop and not to shift of a negative charge adjacent to M4.

Deletion of equivalent residues in non-ε subunits

To determine whether the effects of deleting a C-terminal residue of the M3–M4 loop are subunit specific, we constructed corresponding deletion mutants of the α (αH408del), β (βR446del) and δ (δR450del) subunits (Fig. 3C). The β and δ deletion mutants reduce surface expression of AChR to ~5% of wild-type (Fig. 4A) and shorten channel opening events by about the same amount as εN436del (Table 2 and Fig. 5H and I). The αH408del mutation reduces expression of AChR to ~20% of wild-type (Fig. 4A) and, in striking contrast to the β and δ deletion mutants, prolongs the dominant component of open intervals ~3.5-fold and that of bursts ~13.5-fold (Table 2 and Fig. 5G).

Because HEK cells bound similar low levels of [^{125}I]α-bgt after transfection with δR450del-AChR, $\alpha_2\beta\varepsilon_2$-AChR, βR446del-AChR and $\alpha_2\beta\varepsilon_2$-AChR (Fig. 4A), the channel events recorded from the transfected HEK cells could have arisen from δ-omitted or β-omitted receptors rather than from δR450del-AChR or βR446del-AChR. To test this possibility, we expressed either δ- or β-omitted AChRs in HEK cells in each of three different experiments and searched for channel openings in 30 and 31 patches, respectively, but detected no channel openings. Therefore, it is unlikely that either δ- or β-omitted AChRs, if present, are functional.

Activation kinetics of εN436del-AChR and αH408del-AChR

To determine the mechanism by which the εN436del receptor shortens and the α408Hdel receptor prolongs channel opening events, we examined their kinetics of activation at desensitizing concentrations of ACh (see Methods). Wild-type and εN436del-AChRs generated well-defined clusters of openings at ACh concentrations as low as 10 and 20 μM, respectively, but αH408del-AChR produced clusters of openings even at 0.3 μM ACh, indicating an enhanced propensity of receptors containing the mutant α subunit to become desensitized (Fig. 6, left column).

Table 2 *Single-channel recordings of wild-type and mutant AChRs expressed in HEK cells*

	Open interval			Bursts		
	τ_1 (ms) (a_1)	τ_2 (ms) (a_2)	τ_3 (ms) (a_3)	τ_1 (ms) (a_1)	τ_2 (ms) (a_2)	t_3 (ms) (a_3)
Wild-type	0.037 ± 0.033[a]	0.31 ± 0.050	1.35 ± 0.05	0.036 ± 0.002[b]	0.47 ± 0.06	3.31 ± 0.12
	(0.17 ± 0.02)	(0.27 ± 0.04)	(0.67 ± 0.04)	(0.24 ± 0.021)	(0.21 ± 0.03)	(0.58 ± 0.04)
εN436del	0.031 ± 0.0033[c]	0.24 ± 0.06[d]	0.62 ± 0.03	0.036 ± 0.005[c]	0.30 ± 0.03[e]	1.24 ± 0.092
	(0.15 ± 0.01)	(0.46 ± 0.03)	(0.76 ± 0.09)	(0.23 ± 0.022)	(0.43 ± 0.06)	(0.78 ± 0.07)
εD435del	ND	0.20 ± 0.09	0.87 ± 0.05	ND	0.25 ± 0.08	1.66 ± 0.15
		(0.24 ± 0.08)	(0.76 ± 0.08)		(0.35 ± 0.09)	(0.65 ± 0.09)
εDN435del	ND	0.20 ± 0.02	0.88 ± 0.04	ND	0.31 ± 0.07	1.82 ± 0.10
		(0.34 ± 0.06)	(0.66 ± 0.06)		(0.48 ± 0.06	(0.52 ± 0.06)
εN436R	0.058 ± 0.014	0.39 ± 0.08[b]	1.31 ± 0.12	0.052 ± 0.01	0.45 ± 0.13[f]	3.33 ± 0.44
	(0.16 ± 0.008)	(0.29 ± 0.55)	(0.70 ± 0.07)	(0.32 ± 0.02)	(0.25 ± 0.01)	(0.53 ± 0.07)
εN436D	0.054 ± 0.014[b]	0.39 ± 0.10	1.15 ± 0.13	0.034 ± 0.006[f]	0.55 ± 0.15	3.03 ± 0.15
	(0.14 ± 0.07)	(0.23 ± 0.48)	(0.72 ± 0.08)	(0.20 ± 0.08)	(0.26 ± 0.07)	(0.62 ± 0.10)
βR446del	0.032 ± 0.0024[f]	ND	0.73 ± 0.12	0.027 ± 0.004[f]	ND	1.40 ± 0.29
	(0.12 ± 0.0009)		(0.93 ± 0.03)	(0.11 ± 0.03)		(0.84 ± 0.07)
δR450del	0.041[c]	0.33 ± 0.06[f]	0.73 ± 0.12	0.050[c]	0.49 ± 0.12[b]	1.13 ± 0.18
	(0.30)	(0.49 ± 0.11)	(0.60 ± 0.12)	(0.24)	(0.46 ± 0.10)	(0.70 ± 0.10)
αH408del	0.031 ± 0.0030	0.98 ± 0.21	4.70 ± 0.76	0.067 ± 0.02	1.33 ± 0.29	44.76 ± 3.56
	(0.20 ± 0.03)	(0.16 ± 0.03)	(0.68 ± 0.05)	(0.41 ± 0.05)	(0.21 ± 0.05)	(0.38 ± 0.05)

Values indicate mean ± SE. τ_n and a_n indicate time constants and fractional histogram areas. Wild-type, εN436del, εD435del, εN436R, εN436D and αH408del were recorded with 50 nM ACh from 21, 11, 3, 5, 5 and 6 patches, respectively; εDN435del, βR446del and δR450del were recorded with 1 μM ACh from 3, 5 and 7 patches respectively. Membrane potential = −80 mV. [a, b, c, d, e, f]Either the first or the second component was not detected at 12, 3, 6, 7, 8 and 2 patches, respectively.

For both wild-type and εN436del-AChRs, the longest closed-time component shifted to shorter durations with increasing ACh concentration (Fig. 6, central column). The open times of the εN436del receptors were briefer and those of the αH408del receptor longer compared with wild-type (Fig. 6, right column). Dwell times for wild-type and mutant receptors show typical dependence on ACh concentration: closings become briefer with increasing ACh concentration, and the major component of openings changes little across ACh concentrations.

To determine the consequences of the mutations on rate constants underlying receptor activation, we analysed the global set of open and closed dwell times according to scheme 1:

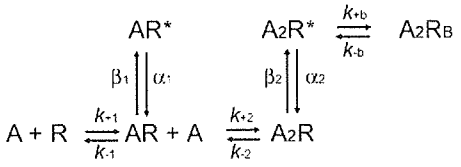

In this scheme, two agonists (A) bind to the receptor (R) with association rate constants k_{+1} and k_{+2}, and dissociate with rate constants k_{-1} and k_{-2}. Receptors occupied by one agonist open with rate β_1 and close with rate α_1, while receptors occupied by two agonists open with rate β_2 and close with rate α_2. Asterisks indicate open states and R_B indicates the blocked state of the receptor. At high ACh concentrations, ACh blocks the open channel with rate k_{+b}, and the channel unblocks with rate k_{-b}. The fitted rate constants allow calculation of the equilibrium dissociation constants ($K_n=k_{-n}/k_{+n}$, $K_B=k_{-b}/k_{+b}$) and the channel gating equilibrium constants ($\theta_n=\beta_n/\alpha_n$). This scheme allows for only two open states, whereas low-concentration recordings (Fig. 5 and Table 2) had revealed three open states. However, at the high concentrations of ACh required to elicit clusters of channel events due to a single channel, only two components of openings are observed, presumably because the briefest class of monoliganded openings occurs too infrequently to be identified.

Scheme 1 provided a good description of the closed and open intervals for wild-type and εN436del receptors but did not provide a satisfactory description of the closed intervals for the αH408del mutant. The chief problem was complexity of the closed duration distribution, which exhibited at least one more component than accounted for by scheme 1. We therefore examined alternative scheme 2, which incorporated an additional closed state branching from the diliganded open state:

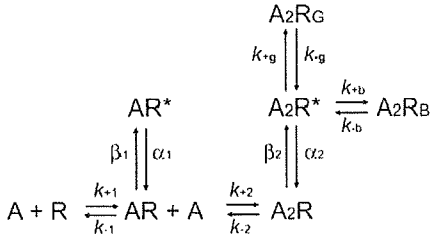

An analogous brief closed state was suggested by Elenes and Auerbach (2002) for wild-type mouse muscle AChR, and by Hatton and colleagues in describing the activation of the εL221F slow-channel mutation (Hatton *et al.*, 2003), both groups suggesting that it corresponded to a short-lived

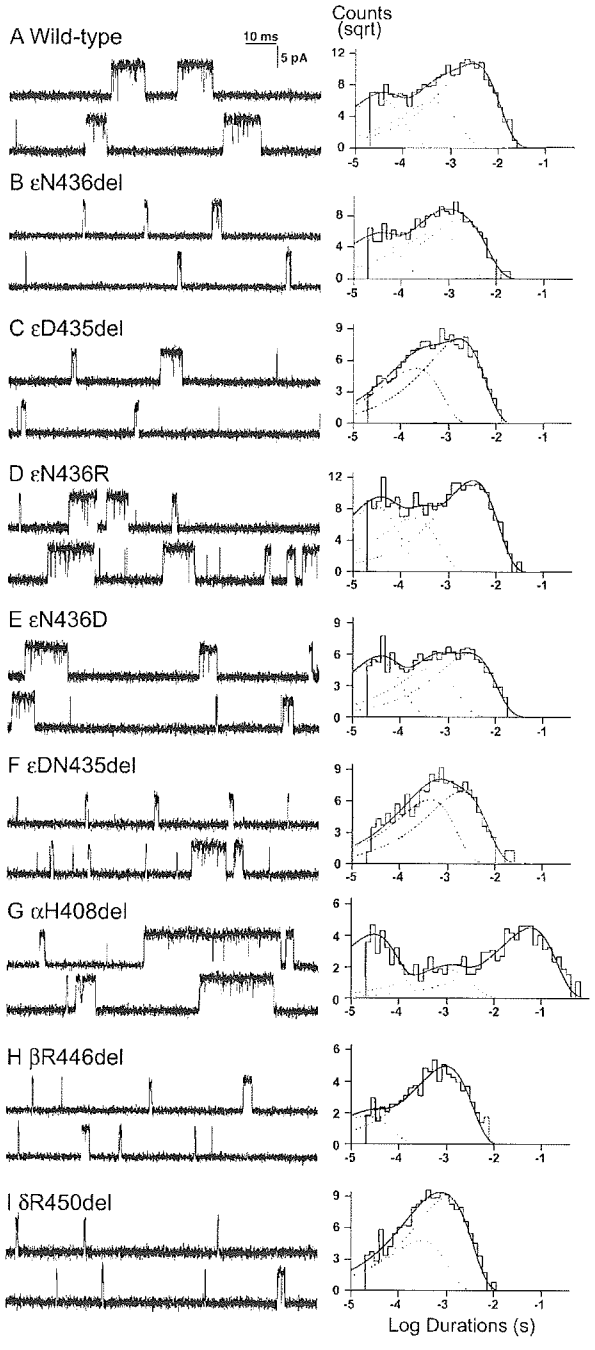

Fig. 5 (*Left*) AChR channel events elicited by 50 nM (A, B, C, D, E, G) or 1 μM (F, H, I) ACh from HEK cells transfected with indicated AChR subunits. (*Right*) Burst duration histograms fitted to the sum of exponentials.

desensitized state. Schemes 1 and 2 provided equally satisfactory fits and similar rate constants for the human wild-type and εN436del receptors. To compare activation kinetics of wild type and mutant receptors, we analysed our data according to scheme 2 (Table 3).

Table 3 *Kinetic parameters of wild-type and mutant AChRs expressed in HEK cells*

Rate constant	Wild-type	εN436del	αH408del
k_{+1}	59 ± 6	32 ± 2	72 ± 5
k_{-1}	953 ± 57	414 ± 44	336 ± 41
k_{+2}	77 ± 2	54 ± 1	369 ± 35
k_{-2}	10 300 ± 170	15 800 ± 327	2880 ± 153
β_1	146 ± 13	556 ± 29	194 ± 21
α_1	3240 ± 323	5520 ± 243	19 200 ± 1321
β_2	52 800 ± 1190	42 300 ± 1960	81 900 ± 3037
α_2	2100 ± 69	4000 ± 139	704 ± 39
k_{+g}	20 ± 1	51 ± 6	52 ± 3
k_{-g}	802 ± 62	959 ± 86	10 500 ± 778
k_{+b}	17 ± 2	25 ± 3	ND
k_{-b}	84 100 ± 1719	73 400 ± 5360	ND
K_1 (μM)	16	13	5
K_2 (μM)	133	293	8
θ_1	0.045	0.100	0.010
θ_2	25	11	116
K_B (mM)	4.95	2.93	–
K_G	40	19	202
Predicted burst length (ms)	3.12	1.26	42.40
Low-concentration burst length (ms)	3.31	1.24	44.76

Association rates and k_{+b} are in $\mu M^{-1} s^{-1}$; all other rate constants are in s^{-1}. Gating equilibrium constants θ_n are the ratios β_n/α_n. The predicted burst length was derived from a rate constant Q matrix (Colquhoun and Sigworth, 1995; Colquhoun and Hawkes, 1995). $K_G = k_{-g}/k_{+g}$. ND = not detected.

The fitted rate constants in Table 3 indicate the following functional consequences of the εN346del mutant: by decreasing k_{+2} and increasing k_{-2}, it increases K_2 ~2.2-fold, thus decreasing the affinity of the diliganded closed receptor for ACh; and by decreasing β_2 and increasing α_2, it decreases the gating efficiency of the diliganded receptor (θ_2) ~2.3-fold. The fitted rate constants were used to predict burst duration at very low concentrations of agonist, which agreed very well with the independently determined burst duration obtained at 50 nM ACh (Table 3). Overall, the εN346del burst duration is reduced to 40% of wild-type, and the mutant receptor has mild fast-channel properties (Engel *et al.*, 2003).

The αH408del mutation, on the other hand, has opposite effects to εN346del: by increasing k_{+1} and k_{+2} and decreasing k_{-1} and k_{-2}, it decreases K_1 3-fold and K_2 ~17-fold, thus markedly enhancing both monoliganded and diliganded closed state affinities; by increasing β_2 ~1.5-fold and slowing α_2 ~3.0-fold, it increases the gating efficiency of the diliganded receptor ~5-fold. Again, burst duration predicted by the fitted rate constants agreed well with the independently determined burst duration obtained at 50 nM ACh (Table 3). Burst duration increases ~14-fold, and the αH408del receptor has pronounced slow-channel properties (Engel, *et al.*, 2003).

Figure 7 shows plots of open probabilities (P_{open}) within defined clusters of channel events at different concentrations

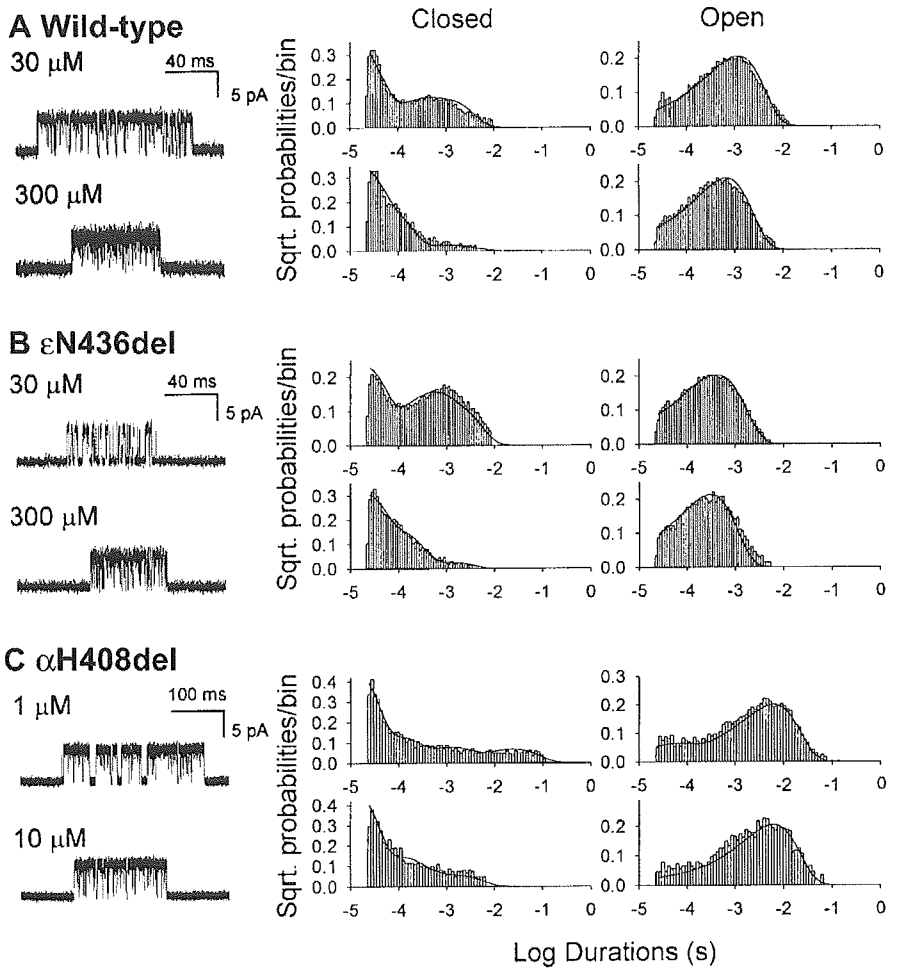

Fig. 6 Kinetics of activation of wild-type (**A**), εN436del- (**B**), and αH408del- (**C**) AChR. (*Left column*) individual clusters of single-channel currents recorded at indicated ACh concentrations from HEK cells. (*Centre and right columns*) Corresponding histograms of closed and open durations with superimposed probability density functions for scheme 2 of receptor activation for the entire range of ACh concentrations. Table 3 shows the fitted rate constants.

of ACh for the wild-type, εN436del-AChR and αH408del receptors. The plotted points are well described by the theoretical P_{open} curve computed from the rate constants determined by fitting scheme 2 to the dwell times (Fig. 7). The P_{open} curve for εN436del receptor is right-shifted with respect to wild-type, indicating a 3.5-fold decreased probability of opening at the EC_{50}. In contrast, the P_{open} curve for the αH408del receptor is left-shifted with respect to wild-type, indicating a ~31-fold increased probability of opening at EC_{50}.

Discussion

Phenotypic consequences of εN436del

Both CMS patients carry the εN436del mutation plus a null mutation in the second ε allele; therefore, εN346del determines the phenotype. EP studies demonstrate severe AChR deficiency, compensatory expression of fetal-type γ-AChR, and short opening events of the expressed adult ε-AChRs. Expression of γ-AChR at the EP has been documented with low-expressor or null mutations of the ε subunit, where it probably serves as a means of phenotypic rescue (Engel *et al.*, 2003). Because the number of AChRs at both patients' EPs is only ~10% of normal and most expressed AChRs harbour the fetal γ subunit, neuromuscular transmission is primarily compromised by the AChR deficiency, and this is compounded by the fast-channel kinetics of the εN436del-AChRs.

Expression of εN436del-AChR in HEK cells was 50% of wild-type. Higher AChR expression in HEK cells than at the EP has been observed previously with other low-expressor missense mutations of AChR (Milone *et al.*, 1998; Ohno *et al.*, 1997; Shen *et al.*, 2002; Wang *et al.*, 1999). This may be due to differences in the rate of synthesis or destruction of the mutant receptor in muscle fibres versus HEK cells. Interaction with the cytoplasmic anchoring protein rapsyn, absent in HEK cells, may also be compromised by the mutant receptors at the EP.

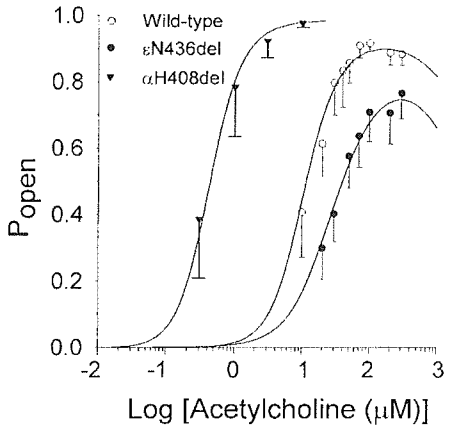

Fig. 7 Open probability (P_{open}) as a function of ACh concentration. Symbols represent mean P_{open} computed for 18–311 clusters per patch. Error bars indicate the standard deviation. Smooth curves are the predicted P_{open} computed from the rate constants in Table 3. Note the right shift of the curve for εN436del and δR450del, and the left shift of the curve for αH408del.

Expression of AChRs harbouring C-terminal deletion mutants of M3–M4 loops

All three C-terminal deletion mutants of the ε M3–M4 loop (εN436del, εD435del and εDN435del) as well as the corresponding deletion mutants of the α (α408Hdel), β (βR446del) and δ (δR450del) subunits curtail surface expression of AChR, whereas the two C-terminal charge mutants of the ε M3–M4 loop (εN436D or εN436R) do not; therefore the decreased AChR expression probably stems from shortening of the M3–M4 loop. Decreased AChR expression, in turn, may stem from abnormal folding and accelerated destruction of nascent peptides in the endoplasmic reticulum, or because C-terminal residues of the M3–M4 loops are required for efficient subunit assembly, or both.

Activation kinetics of C-terminal deletion mutants of the M3–M4 loops

Scheme 1 described well the kinetics of activation the wild-type and εN436del receptors, but did not account for all closed states of the αH408del receptor. We therefore explored an alternative scheme (scheme 2) that allowed an additional closed state connected to the open state of the receptor (A_2R_G); scheme 2 described both closed and open times of the αH408del receptor. Interestingly, applying scheme 2 to the wild-type and the εN436del receptors did not significantly alter the rate constants of activation or improve the likelihood of the fitted parameters compared to scheme 1. This finding differs from that in the mouse receptor, where allowing a non-conducting gap to arise from the diliganded open state improved the quality of the fit (Elenes and Auerbach, 2002). The functional significance of the A_2R_G state is not known; it may represent a brief desensitized state of the receptor (Salamone *et al.*, 1999), but that the dwell in the A_2R_G state is ~13 times shorter for the desensitization prone αH408del receptor than for the wild-type or the εN436del receptor appears inconsistent with this interpretation.

The results shed new light on the structure–function relationships of the AChR. In particular, the M3–M4 linker has been shown to be a primary determinant of the fetal-to-adult kinetic switch, conferred by change from γ to ε subunits (Bouzat *et al.*, 1994), as well as a determinant of the fidelity of channel gating (Milone *et al.*, 1998; Wang, *et al.*, 2000). The collective studies point to γ and ε as subunits that specifically contribute to activation kinetics, but the present work is the first to show a contribution of the M3–M4 loop of the α subunit. The single residue deletion from the α subunit prolongs channel activation episodes and enhances desensitization to extents comparable to severe slow channel mutations. The enhanced activation is attributed to enhanced affinity of ACh for the resting closed state of the receptor as well as to enhanced gating. Both the ACh binding site (Celie *et al.*, 2004) and the channel gate (Miyazawa *et al.*, 2003) are distant from the M3–M4 linker, indicating an allosteric contribution of the M3–M4 loop of the α subunit to receptor function. Thus, combined clinical, morphological, electrophysiological and genetic studies of our two patients unravelled the pathophysiological basis of a CMS. Further experimentation revealed subunit-specific contributions of C-terminal residues of the M3–M4 loops of AChR that allosterically affect gating of the ion channel and ACh occupancy of the more distant binding site.

Acknowledgements

This work was supported by NIH grants to A. G. E. (NS-6277) and to S. M. S. (NS-31744) and by a Muscular Dystrophy Association Grant to A. G. E.

References

Bouzat C, Bren N, Sine SM. Structural basis of different gating kinetics of fetal and adult acetylcholine receptors. Neuron 1994; 13: 1395–402.

Brengman JM, Ohno K, Milone M, Friedman RL, Feldman RG, Engel AG. Identification and functional characterization of eight novel acetylcholine receptor mutations in six congenital myasthenic syndrome kinships. Neurology 2000; 54 (Suppl. 3): A182–3.

Celie PH, van Rossum-Fikkert SE, van Dijk WJ, Brejc K, Smit AB, Sixma TK. Nicotine and carbamycholine binding to nicotinic acetylcholine receptors as studied in AChBP crystal structures. Neuron 2004; 41: 907–14.

Colquhoun D, Hawkes AG. A Q-matrix cookbook: how to write only one program to calculate the single-channel and macroscopic predictions for any kinetic mechanism. In: Sakmann B, Neher E, editors. Single-channel recording. New York: Plenum Press; 1995. p. 589–633.

Colquhoun D, Sakmann B. Fast events in single channel currents activated by acetylcholine and its analogues at the frog muscle end-plate. J Physiol (Lond) 1985; 369: 501–57.

Colquhoun D, Sigworth FJ. Fitting and statistical analysis of single-channel records. In: Sakmann B, Neher E, editors. Single-channel recording. New York: Plenum Press; 1995. p. 483–587.

Croxen R, Young C, Slater C, Haslam S, Brydson M, Vincent A, et al. Endplate γ- and ε subunit mRNA levels in AChR deficiency syndrome due to ε subunit null mutations. Brain 2001; 124: 1362–72.

Elenes S, Auerbach A. Desensitization of diliganded mouse muscle nicotinic acetylcholine receptor channels. J Physiol (Lond) 2002; 541: 367–83.

Engel AG. Quantitative morphological studies of muscle. In: Engel AG, Franzini-Armstrong C, editors. Myology. New York: McGraw-Hill; 1994a. p. 1018–45.

Engel AG. The muscle biopsy. In: Engel AG, Franzini-Armstrong C, editors. Myology. New York: McGraw-Hill; 1994b. p. 822–31.

Engel AG, Nagel A, Walls TJ, Harper CM, Waisburg HA. Congenital myasthenic syndromes. I. Deficiency and short open-time of the acetylcholine receptor. Muscle Nerve 1993; 16: 1284–92.

Engel AG, Lindstrom JM, Lambert EH, Lennon VA. Ultrastructural localization of the acetylcholine receptor in myasthenia gravis and in its experimental autoimmune model. Neurology 1977; 27: 307–15.

Engel AG, Ohno K, Sine SM. Sleuthing molecular targets for neurological diseases at the neuromuscular junction. Nat Rev Neurosci 2003; 4: 339–52.

Gensler S, Sander A, Korngreen A, Traina G, Giese G, Witzemann V. Assembly and clustering of acetylcholine receptors containing GFP-tagged ε or γ subunits. Selective targeting to the neuromuscular junction *in vivo*. Eur J Biochem 2001; 268: 2209–17.

Hatton CJ, Shelley C, Brydson M, Beeson D, Colquhoun D. Properties of the human muscle nicotinic receptor, and of the slow-channel myasthenic syndrome mutant εL221F, inferred from maximum likelihood fits. J Physiol (Lond) 2003; 547: 729–60.

Huebsch KA, Maimone MM. Rapsyn-mediated clustering of acetylcholine receptor subunits requires the major cytoplasmic loop of the receptor subunits. J Neurobiol 2003; 54: 486–501.

Hutchinson DO, Walls TJ, Nakano S, Camp S, Taylor P, Harper CM, et al. Congenital endplate acetylcholinesterase deficiency. Brain 1993; 116: 633–53.

Le Novère N, Corringer PJ, Changeux J-P. Improved secondary structure predictions for a nicotinic receptor subunit: incorporation of solvent accessibility and experimental data into a two-dimensional representation. Biophys J 1999; 76: 2329–45.

Luther MA, Schoepfer R, Whiting P, Casey B, Blatt Y, Montal MS, et al. A muscle acetylcholine receptor is expressed in the human cerebellar medulloblastoma cell line TE671. J Neurosci 1989; 9: 1082–96.

Maimone MM, Merlie JP. Interaction of the 43 kd postsynaptic protein with all subunits of the muscle nicotinic acetylcholine receptor. Neuron 1993; 11: 53–66.

Milone M, Hutchinson DO, Engel AG. Patch-clamp analysis of the properties of acetylcholine receptor channels at the normal human endplate. Muscle Nerve 1994; 17: 1364–9.

Milone M, Wang H-L, Ohno K, Prince RJ, Shen X-M, Brengman JM, et al. Mode switching kinetics produced by a naturally occurring mutation in the cytoplasmic loop of the human acetylcholine receptor ε subunit. Neuron 1998; 20: 575–88.

Milone M, Shen X-M, Ohno K, Harper CM, Fukudome T, Stilling G, et al. Unusual congenital myasthenic syndrome with endplate AChR deficiency caused by alpha subunit mutations and a remitting-relapsing course. Neurology 1999; 52 Suppl. 2: 185–6.

Miyazawa A, Fujiyoshi Y, Unwin N. Nicotinic acetylcholine receptor at 4.6 Å resolution: transverse tunnels in the channel wall. J Mol Biol 1999; 288: 765–86.

Miyazawa A, Fujiyoshi Y, Unwin N. Structure and gating mechanism of the acetylcholine receptor pore. Nature 2003; 423: 949–55.

Ohno K, Wang H-L, Milone M, Bren N, Brengman JM, Nakano S, et al. Congenital myasthenic syndrome caused by decreased agonist binding affinity due to a mutation in the acetylcholine receptor ε subunit. Neuron 1996; 17: 157–70.

Ohno K, Quiram P, Milone M, Wang H-L, Harper CM, Pruitt JN, et al. Congenital myasthenic syndromes due to heteroallelic nonsense/missense mutations in the acetylcholine receptor ε subunit gene: identification and functional characterization of six new mutations. Hum Mol Genet 1997; 6: 753–66.

Ohno K, Milone M, Shen X-M, Engel AG. A frameshifting mutation in CHRNE unmasks skipping of the preceding exon. Hum Mol Genet 2003; 12: 3055–66.

Plomp JJ, van Kempen GTH, Molenaar PC. Adaptation of quantal content to decreased postsynaptic sensitivity at single endplates in α-bungarotoxin treated rats. J Physiol (Lond) 1992; 458: 487–99.

Plomp JJ, van Kempen GTH, De Baets MB, Graus YMF, Kuks JBM, Molenaar PC. Acetylcholine release in myasthenia gravis: regulation at single end-plate level. Ann Neurol 1995; 37: 627–36.

Popot JL, Changeux J-P. Nicotinic receptor of acetylcholine: structure of an oligomeric integral membrane protein. Physiol Rev 1984; 64: 1162–239.

Qin F, Auerbach A, Sachs F. Estimating single-channel kinetic parameters from idealized patch-clamp data containing missed events. Biophys J 1996; 70: 264–80.

Quiram P, Ohno K, Milone M, Patterson MC, Pruitt NJ, Brengman JM, et al. Mutation causing congenital myasthenia reveals acetylcholine receptor β/δ subunit interaction essential for assembly. J Clin Invest 1999; 104: 1403–10.

Salamone FN, Zhou M, Auerbach A. A re-examination of adult mouse nicotinic acetylcholine receptor channel activation kinetics. J Physiol (Lond) 1999; 516: 315–30.

Schoepfer R, Luther MA, Lindstrom J. The human medulloblastoma cell line TE671 expresses a muscle-like acetylcholine receptor. Cloning of the alpha-subunit cDNA. FEBS Lett 1988; 226: 235–40.

Shen X-M, Ohno K, Fukudome T, Tsujino A, Brengman JM, De Vivo DC, et al. Congenital myasthenic syndrome caused by low-expressor fast-channel AChR δ subunit mutation. Neurology 2002; 59: 1881–8.

Shen X-M, Ohno K, Tsujino A, Brengman JM, Gingold M, Sine SM, et al. Mutation causing severe myasthenia reveals functional asymmetry of AChR signature Cys-loops in agonist binding and gating. J Clin Invest 2003; 111: 497–505.

Sieb JP, Kraner S, Rauch M, Steinlein OK. Immature end-plates and utrophin deficiency in congenital myasthenic syndrome caused by epsilon-AChR subunit truncating mutations. Hum Genet 2000; 107: 160–4.

Sigworth FJ, Sine SM. Data transformation for improved display and fitting of single-channel dwell time histograms. Biophys J 1987; 52: 1047–54.

Sine SM. Molecular dissection of subunit interfaces in the acetylcholine receptor: identification of residues that determine curare selectivity. Proc Natl Acad Sci USA 1993; 90: 9436–40.

Sine SM, Taylor P. Functional consequences of agonist mediated state transitions in the cholinergic receptor. Studies in cultured muscle cells. J Biol Chem 1979; 254: 3315–25.

Uchitel O, Engel AG, Walls TJ, Nagel A, Atassi ZM, Bril V. Congenital myasthenic syndromes. II. A syndrome attributed to abnormal interaction of acetylcholine with its receptor. Muscle Nerve 1993; 16: 1293–301.

Wang H-L, Milone M, Ohno K, Shen X-M, Tsujino A, Batocchi AP, et al. Acetylcholine receptor M3 domain: stereochemical and volume contributions to channel gating. Nat Neurosci 1999; 2: 226–33.

Wang H-L, Ohno K, Milone M, Brengman JM, Evoli A, Batocchi AP, et al. Fundamental gating mechanism of nicotinic receptor channel revealed by mutation causing a congenital myasthenic syndrome. J Gen Physiol 2000; 116: 449–60.

Yu X-M, Hall ZW. The role of the cytoplasmic domains of individual subunits of the acetylcholine receptor in 43 kDa protein-induced clustering in COS cells. J Neurosci 1994; 14: 785–95.

Acta Myologica • 2005; XXIV: p. 50-54

Splicing abnormalities in congenital myasthenic syndromes

KINJI OHNO[1, 2], ANDREW G. ENGEL[2]

[1]*Division of Neurogenetics and Bioinformatics, Department of Advanced Medical Science, Nagoya University Graduate School of Medicine, Nagoya, Japan;*
[2]*Department of Neurology, Mayo Clinic, Rochester, MN, USA*

A total of 173 mutations has been reported to date in eight genes in congenital myasthenic syndromes. Sixteen intronic and five exonic mutations in three genes affect pre-mRNA splicing. Eight of these are of particular interest, and are reviewed in this article.

An A-to-G mutation at intron position +3 results in exon skipping only when there are mismatched nucleotides to U1 snRNA at positions +4 to +6. Similarly, a mutation at the last nucleotide of an exon causes exon skipping when a nucleotide at position +6 is not complementary to U1 snRNA. We observe the similar compensation mechanisms for mismatches to U1 snRNA at 179,917 native human splice donor sites.

A 7-bp deletion in *CHRNE* exon 7 causes skipping of the preceding 101-bp exon 6. We found in general that the nonsense-mediated altered splicing of a remote exon (NASRE) is mediated by inherent weak splicing signals flanking the skipped exon and degradation of a normally spliced transcript by the nonsense-mediated mRNA decay (NMD).

A 16-bp duplication spanning the *CHRNE* intron 10/exon 11 boundary generates two copies of 3' splice sites, and the downstream copy is exclusively silenced. Analysis of a series of artificial mutants conforms to the scanning model of recognition of the 3' splice site that predicts that the first 'ag' more than 13 nucleotides downstream of the branch point is selected for splicing.

Splicing mutations may be more frequent than suspected, and one must always be aware of possible splicing abnormalities when analyzing human mutations.

Key words: aberrant splicing, congenital myasthenic syndromes

Introduction

Congenital myasthenic syndromes (CMS) are monogenic disorders caused by genetic defects of molecules expressed at the neuromuscular junction. We identified genetic defects in (i) *CHAT* encoding choline acetyltransferase that resynthesizes acetylcholine at the nerve terminal [1], (ii) *COLQ* encoding the collagenic tail subunit of asymmetric acetylcholinesterase (AChE) [2], (iii) *RAPSN* encoding rapsyn that clusters acetylcholine receptor (AChR) at the endplate [3], (iv) *CHRNA1*, *CHRNB1*, *CHRND*, *CHRNE* encoding AChR α, β, δ, and ε subunits, respectively [4], and (v) *SCN4A* encoding skeletal muscle voltage-gated sodium channel [5]. Mutations in AChR subunit genes cause AChR deficiency, fast channel syndrome, or slow channel syndrome. AChR mutations causing the slow channel syndrome are transmitted as a dominant trait, whereas all other CMS mutations are recessive.

A total of 173 mutations has been reported to date in *CHAT, COLQ, RAPSN, CHRNA1*, *CHRNB1*, *CHRND*, *CHRNE*, and *SCN4A* in CMS [6]. Twenty-one mutations (16 intronic and 5 exonic mutations) in *COLQ, CHRNE,* and *RAPSN* affect pre-mRNA splicing (Table 1). In *COLQ*, there are three intronic and one exonic mutations affecting pre-mRNA splicing. In *CHRNE*, 13 mutations affecting intron/exon boundaries and 3 exonic mutations cause aberrant splicing. Eight out of the 21 mutations are of particular interest, and are reviewed in this article.

1. G at intron position +3 is compensated for by matched nucleotides to U1 snRNA at positions +4 to +6

An A-to-G substitution at position +3 of *COLQ* intron 16 (IVS16+3A>G) results in skipping of

Address for correspondence: Kinji Ohno, MD, PhD, Division of Neurogenetics and Bioinformatics, Department of Advanced Medical Science, Nagoya University Graduate School of Medicine, 65 Tsurumai, Showa, Nagoya 466-8550, JAPAN. Tel. +81-52-744-2446; Fax +81-52-744-2449. E-mail: ohnok@med.nagoya-u.ac.jp

Table 1. Splicing mutations observed in congenital myasthenic syndromes.

GENE	MUTATION	EXON/INTRON	STATEMENTS IN TEXT*	REFERENCE
COLQ	g.IVS1-1G>A	Intron 1		[19]
	g.IVS15+1G>A	Intron 15		[20]
	g.IVS16+3A>G	Intron 16	1	[7]
	p.E415G	Exon 16	4	[11]
CHRNE	g.IVS4+1G>A	Intron 4		[21]
	g.IVS4-2A>C	Intron 4		[10]
	g.IVS6+1G>T	Intron 6		[22]
	g.IVS6-1G>C	Intron 6		[8]
	g.IVS7+2T>C	Intron 7		[23, 24]
	g.IVS7-2A>G	Intron 7		[25]
	g.IVS9+1G>T	Intron 9		[26]
	g.IVS9-1G>C	Intron 9		[10, 27]
	g.IVS9-1G>A	Intron 9		[8]
	g.IVS10-9_c.1167dup16	Intron 10/Exon 11	5	[8]
	g.IVS10+2T>G	Intron 10		[28]
	c.1259_g.IVS11+15del23	Exon 11/Intron 11		[8]
	p.E154X (c.460G>T)	Exon 6	4	[10]
	p.EF157V (c.470delAGT)	Exon 6	4	[10]
	c.553del7	Exon 7	3	[10]
	p.R286M(c.857G>T)	Exon 8	2	[8]
RAPSN	g.IVS4-2A>G	Intron 4		[29]

* Numbers refer to those in the subheadings of the text.

exon 16. This was unexpected, because both A and G are equally frequent at intron position +3 in human genes (Table 2). In pre-mRNA splicing, 9 nucleotides of U1 snRNA base-pair with the splice donor site comprising 3 exonic and 6 intronic nucleotides. The mutation in *COLQ* intron 16 presents mismatched nucleotides to U1 snRNA at positions –3, -2, +3, +4, and +6. Introduction of a nucleotide complementary to U1 snRNA- either at position +4 or +6 results in normal splicing even with a mutant G at position +3. On the other hand, introduction of a nucleotide complementary to U1 snRNA either at position –3 or –2 does not correct splicing. Consistent with a role of residues at +4 to +6 in splicing, analysis of 179,917 native human splice donor sites revealed that with a G at position +3, human genes frequently carry U1 snRNA-complementary nucleotides at positions +4 to +6 (Table 2). Analysis of 11 disease-associated A-to-G mutations at position +3 also indicates that 2 of 3 nucleotides at positions +4 to +6 fail to base-pair, and that the nucleotide at +4 never base-pairs, with U1 snRNA. These data all point to a notion that with G at intron position +3, normal splicing depends on concordance of residues at +4 to +6 with U1 snRNA [7].

2. A mutation at the last nucleotide of an exon results in exon skipping when a nucleotide at intron position +6 is not complementary to U1 snRNA

A single nucleotide substitution at the last nucleotide of *CHRNE* exon 8 (c.857G>T) predicts an Arg-to-Met substitution at codon 286 (p.R286M). By analyzing the cloned entire genomic segment of *CHRNE*, we found that this mutation results in skipping of exon 8. Analysis of 179,917 native human splice donor sites revealed that a mismatch to U1 snRNA at the last nucleotide of an exon is frequently compensated for by a matched nucleotide at intron position +6, and also but to a lesser extent by nucleotides at +4 and +5 (Table 2). Indeed, 19 out of 28 splicing mutations reported to date at the last G nucleotide of an exon do not carry a matched T nucleotide at position +6. In the remaining 7 mutants carrying a matched T nucleotide at position +6, one or two mismatches to U1 snRNA are observed at intron positions +4 and +5 [8].

An extreme example of this notion is observed in *IKBKAP* IVS20+6T>C causing familial dysau-

Table 2. Nucleotide frequencies at positions –3 to +6 of 179,917 native human splice donor sites.

	% OF NUCLEOTIDE AT POSITION								
	-3	-2	-1	+1	+2	+3	+4	+5	+6
Whole splice donor sites (179,917 sites)									
A	33.2	*62.9*	10.2	0.0	0.0	*59.2*	*68.8*	9.0	17.9
C	*36.1*	11.1	3.0	0.0	0.0	3.0	7.7	6.0	15.3
G	18.5	11.9	*79.6*	*100.0*	0.0	34.8	12.0	*77.2*	19.5
T	12.2	14.1	7.2	0.0	*100.0*	3.0	11.5	7.8	*47.2*
Splice donor sites with A at position +3 (106,541 sites)									
A	34.7	*64.9*	11.6	0.0	0.0	*100.0*	*63.8*	13.0	21.9
C	*34.8*	9.5	2.5	0.0	0.0	0.0	9.0	7.9	14.1
G	17.6	11.3	*78.7*	*100.0*	0.0	0.0	12.5	*67.9*	20.1
T	13.0	14.3	7.2	0.0	*100.0*	0.0	14.7	11.2	*43.9*
Splice donor sites with G at position +3 (62,544 sites)									
A	30.3	*56.9*	8.6	0.0	0.0	*0.0*	*80.0*	3.0	12.1
C	*37.4*	14.8	4.1	0.0	0.0	0.0	5.7	3.1	17.7
G	20.5	13.4	*79.3*	*100.0*	0.0	100.0	10.6	*91.5*	19.3
T	11.8	14.9	8.0	0.0	*100.0*	0.0	3.7	2.3	*50.9*
Splice donor sites with G at position -1 (143,251 sites)									
A	32.9	*67.8*	0.0	0.0	0.0	*58.5*	*65.0*	10.7	20.4
C	*37.9*	6.6	0.0	0.0	0.0	3.4	8.7	6.8	16.7
G	18.2	10.6	*100.0*	*100.0*	0.0	34.6	13.7	*73.1*	22.6
T	10.9	15.0	0.0	0.0	*100.0*	3.5	12.5	9.3	*40.3*
Splice donor sites with non-G at position -1 (36,666 sites)									
A	34.1	*43.9*	49.9	0.0	0.0	*61.9*	*83.6*	2.5	8.5
C	*28.7*	28.8	14.9	0.0	0.0	1.4	3.8	2.7	9.8
G	19.9	16.8	*0.0*	*100.0*	0.0	35.3	5.4	*92.9*	7.7
T	17.2	10.5	35.3	0.0	*100.0*	1.4	7.3	1.9	*74.0*

Underlines indicate high frequencies of complementary nucleotides to U1 snRNA at positions +4 to +6 when there is G at position +3 or non-G at position –1. The data were extracted from the Human Genome Database Build 35.1. Nucleotides complementary to U1 snRNA are italicized.

tonomia [9], in which the only mismatched nucleotide at the native splice donor site is A at position –1, and an additional mismatch mutation at position +6 a is enough to cause exon skipping.

Knowledge of compensatory mechanisms at human splice donor sites, allows one to predict the splicing consequences of identified mutations.

3. Nonsense-mediated altered splicing of a remote exon (NASRE)

A 7-bp deletion in *CHRNE* exon 7 (c.553del7) causes skipping of a preceding 101-bp exon 6. This was unexpected, because current models of pre-mRNA splicing cannot explain skipping of a remote exon. A series of artificial mutations expressed in COS cells suggested that presence of a premature termination codon (PTC) determines the splicing consequences. We thus inhibited the nonsense-mediated mRNA decay (NMD) by anisomycin, and found that exon 6 is skipped even in the wild-type *CHRNE* due to weak splicing signals flanking exon 6. The exon-skipped transcript, however, carries a premature stop codon (PTC) in exon 7, and is degraded by NMD. In the presence of a 7-bp deletion in exon 7, the normally spliced transcript carries a PTC in exon 7, and is degraded by NMD. On the other hand, the exon 6-skipped transcript resumes the open reading frame after the 7-bp deletion, and is immune to NMD. The c.553del7 mutation does not directly affect pre-mRNA splicing, but instead swaps the NMD target by placing a PTC in the normally spliced transcript and by removing a PTC from the exon 6-skipped transcript. We found that inherent weak splicing signals and swapping of the NMD target are the common mechanisms observed in nonsense-mediated altered splicing of a remote exon (NASRE) in other genes as well [10].

Skipping of a remote exon has been reported only in four genes, likely because only few researchers look for aberrant splicing of a remote exon. Screen-

ing for aberrant splicing affecting a remote exon, however, is very important, because it potentially converts a "frameshift" to an "inframe" mutation, or vice versa, and thus changes a phenotypic consequence.

4. Exonic splicing enhancer (ESE)-disrupting mutations

Transplantation of recombinant human asymmetric AChE carrying E415G in collagen Q to the frog endplate indicates that E415G does not compromise anchoring of AChE to the synaptic basal lamina. Analysis of muscle mRNA and minigene constructs in COS cells revealed that E415G disrupts an ESE and hence causes skipping of exon 16 [11].

Studies of NASRE mentioned above revealed that *CHRNE* exon 6 carries weak splicing signals. As exons flanked by weak splicing signals frequently harbor ESEs [12], we examined if any of four mutations in *CHRNE* exon 6 observed in CMS patients affects splicing of exon 6. We indeed found that a single nucleotide substitution predicting a nonsense mutation, p.E154X (c.460G>T), and an inframe deletion, p.EF157V (c.470delAGT), both in exon 6 cause aberrant splicing of exon 6 [10]. Before we identified that p.EF157V is a splicing mutation, we expressed mutant AChR carrying p.EF157V in HEK cells, and found that p.EF157V does not significantly affect the level of AChR expression or the ion channel kinetics.

A recent estimate indicates that 15-20% of missense mutations possibly affect an ESE [13]. We always have to think about a possibility that a given exonic mutation potentially disrupts an exonic splicing enhancer or a silencer, even if the mutant protein shows functional abnormalities and readily explains the disease.

5. The scanning model of recognition of the 3' splice site

A 16-bp duplication spanning the *CHRNE* intron 10/exon 11 boundary (g.IVS10-9_c.1167dup16) generates two copies of 3' splice sites, and the downstream copy is exclusively silenced. The mutation is comprised of duplication of 8 intronic and 8 exonic nucleotides. Analysis of a series of artificial mutants conforms to the scanning model of recognition of the 3' splice site that predicts that the first 'ag' more than 13 nucleotides downstream of the branch point is selected for splicing [14, 15]. Previous reports indicate two exceptions against this rule [16-18]: the first 'ag' dinucleotide is hidden in a stable secondary structure; or two 'ag' dinucleotides that are less than 12 nucleotide apart compete for being recognized by the splicesome. As the 16-bp duplication in *CHRNE* is not applicable to these exceptions, the mutation follows the scanning model of the 3' splice site recognition [8].

Some mutations or polymorphisms close the 3' end of an intron potentially create an 'ag' dinucleotide prior to the native 'ag' splice site. The splicing effects of these mutations/polymorphisms must be carefully examined.

Conclusions

As in other disease-causing mutations affecting pre-mRNA splicing, splicing mutations in CMS are not restricted to the intronic AG-GT dinucleotides. Unusual aberrant splicings reviewed in this article were either detected by chance, or sought after when other assays failed to show any functional abnormalities. Splicing mutations may be more frequent than suspected, and one must always be aware of possible splicing abnormalities when analyzing human mutations.

Acknowledgements

This work was supported by the National Institutes of Health grant NS6277 and by a Muscular Dystrophy Association research grant to A.G.E. and by Grant-in-Aid for Scientific Research on Priority Area "RNA" (KAKENHI 17026016) from the Ministry of Education, Culture, Sports, Science and Technology of Japan to K.O.

References

1. Ohno K, Tsujino A, Shen X-M, et al. Choline acetyltransferase mutations cause myasthenic syndrome associated with episodic apnea in humans. Proc Natl Acad Sci U S A 2001;98:2017-22.
2. Ohno K, Brengman JM, Tsujino A, et al. Human endplate acetylcholinesterase deficiency caused by mutations in the collagen-like tail subunit (ColQ) of the asymmetric enzyme. Proc Natl Acad Sci U S A 1998;95:9654-9.
3. Ohno K, Engel AG, Shen X-M, et al. Rapsyn mutations in humans cause endplate acetylcholine receptor deficiency and myasthenic syndrome. Am J Hum Genet 2002;70:875-85.
4. Ohno K, Wang HL, Milone M, et al. Congenital myasthenic syndrome caused by decreased agonist binding affinity due to a mutation in the acetylcholine receptor ε subunit. Neuron 1996;17:157-70.

5. Tsujino A, Maertens C, Ohno K, et al. Myasthenic syndrome caused by mutation of the *SCN4A* sodium channel. Proc Natl Acad Sci U S A 2003;100:7377-82.
6. Engel AG, Ohno K, Sine SM. Sleuthing molecular targets for neurological diseases at the neuromuscular junction. Nat Rev Neurosci 2003;4:339-52.
7. Ohno K, Brengman JM, Felice KJ, et al. Congenital endplate acetylcholinesterase deficiency caused by a nonsense mutation and an A>G splice-donor-site mutation at position +3 of the collagenlike-tail-subunit gene (*COLQ*): How does G at position +3 result in aberrant splicing? Am J Hum Genet 1999;65:635-44.
8. Ohno K, Tsujino A, Shen X-M, et al. Spectrum of splicing errors caused by *CHRNE* mutations affecting introns and intron/exon boundaries. J Med Genet 2005;42:e53.
9. Slaugenhaupt SA, Mull J, Leyne M, et al. Rescue of a human mRNA splicing defect by the plant cytokinin kinetin. Hum Mol Genet 2004;13:429-36.
10. Ohno K, Milone M, Shen XM, et al. A frameshifting mutation in *CHRNE* unmasks skipping of the preceding exon. Hum Mol Genet 2003;12:3055-66.
11. Kimbell LM, Ohno K, Engel AG, et al. C-terminal and heparin-binding domains of collagenic tail subunit are both essential for anchoring acetylcholinesterase at the synapse. J Biol Chem 2004;279:10997-1005.
12. Fairbrother WG, Yeh RF, Sharp PA, et al. Predictive identification of exonic splicing enhancers in human genes. Science 2002;297:1007-13.
13. Gorlov IP, Gorlova OY, Frazier ML, et al. Missense mutations in hMLH1 and hMSH2 are associated with exonic splicing enhancers. Am J Hum Genet 2003;73:1157-61.
14. Smith CW, Porro EB, Patton JG, et al. Scanning from an independently specified branch point defines the 3' splice site of mammalian introns. Nature 1989;342:243-7.
15. Chen S, Anderson K, Moore MJ. Evidence for a linear search in bimolecular 3' splice site AG selection. Proc Natl Acad Sci U S A 2000;97:593-8.
16. Blasband AJ, Rogers KT, Chen XR, et al. Characterization of the rat transforming growth factor alpha gene and identification of promoter sequences. Mol Cell Biol 1990;10:2111-21.
17. Smith CW, Chu TT, Nadal-Ginard B. Scanning and competition between AGs are involved in 3' splice site selection in mammalian introns. Mol Cell Biol 1993;13:4939-52.
18. Chua K, Reed R. The RNA splicing factor hSlu7 is required for correct 3' splice-site choice. Nature 1999;402:207-10.
19. Ishigaki K, Nicolle D, Krejci E, et al. Two novel mutations in the *COLQ* gene cause endplate acetylcholinesterase deficiency. Neuromuscul Disord 2003;13:236-44.
20. Ohno K, Engel AG, Brengman JM, et al. The spectrum of mutations causing endplate acetylcholinesterase deficiency. Ann Neurol 2000;47:162-70.
21. Sieb JP, Kraner S, Rauch M, et al. Immature end-plates and utrophin deficiency in congenital myasthenic syndrome caused by epsilon-AChR subunit truncating mutations. Hum Genet 2000;107:160-4.
22. Deymeer F, Serdaroglu P, Gulsen-Parman Y, et al. Clinical characteristic of a group of Turkish patients having a benign CMS phenotype with ptosis and marked ophthalmoparesis and mutations in the acetylcholine receptor epsilon subunit gene. Acta Myologica 2000;19:29-32.
23. Ohno K, Anlar B, Özdirim E, et al. Myasthenic syndromes in Turkish kinships due to mutations in the acetylcholine receptor. Ann Neurol 1998;44:234-41.
24. Abicht A, Stucka R, Song I-H, et al. Genetic analysis of the entire AChR ε-subunit gene in 52 congenital myasthenic families. Acta Myologica 2000;19:23-7.
25. Barisic N, Schmidt C, Sidorova OP, et al. Congenital myasthenic syndrome (CMS) in three European kinships due to a novel splice mutation (IVS7 - 2 A/G) in the epsilon acetylcholine receptor (AChR) subunit gene. Neuropediatrics 2002;33:249-54.
26. Croxen R, Young C, Slater C, et al. End-plate gamma- and epsilon-subunit mRNA levels in AChR deficiency syndrome due to epsilon-subunit null mutations. Brain 2001; 124:1362-72.
27. Shen X-M, Ohno K, Sine SM, et al. Subunit-specific contribution to agonist binding and channel gating revealed by inherited mutation in muscle acetylcholine receptor M3-M4 linker. Brain 2005;128:345-55.
28. Middleton L, Ohno K, Christodoulou K, et al. Chromosome 17p-linked myasthenias stem from defects in the acetylcholine receptor epsilon-subunit gene. Neurology 1999;53:1076-82.
29. Richard P, Gaudon K, Andreux F, et al. Possible founder effect of rapsyn N88K mutation and identification of novel rapsyn mutations in congenital myasthenic syndromes. J Med Genet 2003;40:e81.

PAPER

Age associated axonal features in HNPP with 17p11.2 deletion in Japan

H Koike, M Hirayama, M Yamamoto, H Ito, N Hattori, F Umehara, K Arimura, S Ikeda, Y Ando, M Nakazato, R Kaji, K Hayasaka, M Nakagawa, S Sakoda, K Matsumura, O Onodera, M Baba, H Yasuda, T Saito, J Kira, K Nakashima, N Oka, G Sobue

J Neurol Neurosurg Psychiatry 2005;**76**:1109–1114. doi: 10.1136/jnnp.2004.048140

See end of article for authors' affiliations

Correspondence to: Dr Gen Sobue, Department of Neurology, Nagoya University Graduate School of Medicine, Nagoya 466–8550, Japan; sobueg@med.nagoya-u.ac.jp

Received 20 June 2004
Revised version received 28 September 2004
Accepted 18 November 2004

Objective: To clarify age related changes in the clinicopathological features of hereditary neuropathy with liability to pressure palsy (HNPP) in Japanese patients with deletion of 17p11.2, particularly concerning axonal abnormalities.

Methods: Forty eight proband patients from 48 HNPP families were assessed as to clinical, electrophysiological, and histopathological features, including age associated changes beyond those in controls.

Results: Motor conduction studies showed age associated deterioration of compound muscle action potentials in nerves vulnerable to repetitive compression (median, ulnar, and peroneal nerves), but not in others such as the tibial nerve. Sensory conduction studies revealed more profound reduction of action potentials than motor studies with little age related change. Large myelinated fibre loss was seen in the sural nerve irrespective of age at examination.

Conclusions: Irreversible axonal damage may occur at entrapment sites in motor nerves in HNPP patients, progressing with aging. Sensory nerves may show more profound axonal abnormality, but without age association. The electrophysiological features of HNPP are presumed to be a mixture of abnormalities occurring from early in life and acquired features caused by repetitive insults at entrapment sites. Unlike Charcot-Marie-Tooth disease type 1A, age associated axonal damage may not occur unless the nerves are subjected to compression.

Hereditary neuropathy with liability to pressure palsy (HNPP) is an autosomal dominant disorder characterised by recurrent transient nerve palsies associated with compression at the typical anatomic sites of potential nerve entrapment.[1 2] Tomacula, which represent focal thickening of the myelin sheath, characteristically are seen in both sensory and motor nerves in HNPP.[3–6] This disorder usually is associated with a 1.5 Mb deletion of locus 17p11.2, which contains the gene for peripheral myelin protein 22 (PMP22).[7–9] HNPP therefore appears to represent a reciprocal product of Charcot-Marie-Tooth disease type 1A (CMT1A), which is associated with duplication of PMP22.[10] PMP22 is an important factor for regulation of Schwann cell proliferation and apotosis.[11] As the Schwann cell plays an important role in maintenance of the axon, axonal loss associated with demyelination has been reported to occur in patients with CMT1A.[12–15] Age associated reduction of compound muscle action potential (CMAP) amplitude resulting from large-axon loss has been reported in CMT1A[13] and is closely related to clinical manifestations and functional impairment.[14 15]

In Western countries, the clinical and electrophysiological features of HNPP have been described on a large scale.[16–20] Characteristic electrophysiological findings are multifocal slowing of conduction at sites of entrapment, prolonged distal latency (DL), mild slowing of motor nerve conduction velocity (MCV), and diffuse abnormality of sensory nerve conduction velocity (SCV).[16 18–20] However, there have been no similar large scale investigations of the clinical and electrophysiological features of HNPP in Asian subjects. Furthermore, it has not been clarified whether electrophysiological and histopathological abnormalities, particularly axonal features, worsen with aging in HNPP as happens in CMT1A.

The present investigation was carried out in Japan and we studied HNPP including its electrophysiological and histopathological features, especially in relation to aging.

METHODS

Patients and DNA diagnosis

An HNPP survey was conducted by the study group for hereditary neuropathy in Japan under the auspices of the Ministry of Health, Labor, and Welfare.[15 21] A total of 48 proband patients from 48 HNPP families, whose 17p11.2 deletion was confirmed, were investigated. The mean age (SD) of the patients at examination was 41.8 (18.5) years (table 1). All subjects underwent clinical examination by at least one neurologist. Patients with chronic alcoholism or vitamin deficiency were not included. Four patients manifested mild glucose intolerance. To confirm the diagnosis of HNPP, DNA analyses for the presence of a chromosome 17p11.2–12 deletion, which includes a 1.5 Mb region containing the PMP22 gene between CMT1A-REP repeats, were performed in all patients. For most patients these analyses were performed at the Department of Neurology at Nagoya University Graduate School of Medicine as described previously,[22] while DNA was analysed at other institutions for the rest. The characteristic deletion in HNPP was detected by Southern analysis, probing with PMP22 cDNA, and CMT1A-REP fragments as described previously.[22–24] Hybridisation with PMP22 cDNA and pNEA102, pHK1.0P, and pHK5.2 probes, which map within the CMT1A-REP, was carried out

Abbreviations: CMAP, compound muscle action potential; CMT1A, Charcot-Marie-Tooth disease type 1A; DL, distal latency; HNPP, hereditary neuropathy with liability to pressure palsy; MCV, motor nerve conduction velocity; PMP22, peripheral myelin protein 22; SCV, sensory nerve conduction velocity; SNAP, sensory nerve action potential

to determine the gene dose of the 1.5 Mb region containing PMP22. Deletion of one copy of the PMP22 gene, compared to the presence of two copies in normal controls, was genetically identified as HNPP. Informed consent was obtained in all patients, and the study as a whole was approved by the Ethics Committee of Nagoya University Graduate School of Medicine.

Electrophysiological study

Motor and sensory conduction was measured in the median, ulnar, tibial, peroneal, and sural nerves, using a standard method with surface electrodes for stimulation and recording.[25 26] Motor conduction was investigated in the median, ulnar, tibial, and peroneal nerves, recording from the abductor pollicis brevis, abductor digiti minimi, abductor hallucis brevis, and extensor digitorum brevis muscles, respectively. The following nerve segments were used for calculating MCV: wrist to elbow for the median nerve, wrist to distally at the elbow for the ulnar nerve, ankle to popliteal fossa for the tibial nerve, and ankle to distally at the fibular head for the peroneal nerve. Sensory conduction was investigated in the median, ulnar, and sural nerves, using antidromic recording from ring electrodes at the second and fifth digit for the median and ulnar nerves respectively, and bar electrodes at the ankle for the sural nerve. SCV was calculated for the distal segment. Amplitudes of CMAP and sensory nerve action potential (SNAP) were measured from the baseline to the first negative peak. Waveforms also were analysed to assess temporal dispersion. For motor nerves, we measured duration from the onset to the first crossing of the baseline in the CMAP.[27] For sensory nerves, duration from the onset of the SNAP to the first negative peak rather than to the first crossing of the baseline was measured to avoid artefacts from overlapping muscle action potentials.[25] This was necessary because some motor axons have thresholds similar to those of large myelinated sensory axons, resulting in superimposition on the SNAP that modifies the waveform, especially when abnormal nerves are examined.[28 29] Because of a delay at the neuromuscular junction, the initial phase of the waveform of SNAP is less likely to be affected by muscle action potentials than the later phase.[29]

Control values were obtained in 171 normal volunteers (51.0 (SD 16.3) years of age; male:female, 89:82) for the median nerve, 170 (51.2 (SD 16.4) years of age; male:female, 88:82) for the ulnar nerve, 161 (51.8 (SD 16.6) years of age; male:female, 85:76) for the tibial nerve, 171 (54.2 (SD 16.7) years of age; male:female, 92:79) for the peroneal nerve, and 163 (52.2 (SD 16.7) years of age; male:female, 85:78) for the sural nerve.

Table 1 Characteristics of 48 Japanese HNPP probands with deletion of 17p11.2–12

Clinical features	n (%)
Age at onset, years	33.1 (SD 19.3)
Age at examination, years	41.8 (SD 18.5)
Men/women	38/10
Family history	24 (50%)
Athletic impairment during childhood	1 (2%)
Pes cavus or hammer toe	2 (4%)
Atrophy in the legs	6 (13%)
Pattern of neuropathy	
Multiple mononeuropathy	41 (85%)
Symmetric polyneuropathy	7 (15%)
History of transient nerve palsy	
Median nerve	11 (23%)
Ulnar nerve	18 (38%)
Radial nerve	7 (15%)
Peroneal nerve	29 (60%)
Brachial plexus	10 (21%)
Activity of daily living	
Able to walk	46 (96%)
Unable to walk	2 (4%)
Bedridden	0

Age at onset, age at first awareness of neuropathic symptoms; Family history, obvious family history of recurrent transient nerve palsies.

Histopathological study

Sural nerve biopsy was performed in 14 patients as described previously.[30 31] Informed consent was obtained beforehand. Specimens were divided into two portions. The first portion was fixed in 2.5% glutaraldehyde in 0.125 M cacodylate buffer (pH 7.4) and embedded in epoxy resin for morphometric study. The density of myelinated fibres was assessed in toluidine blue stained semithin sections using a computer assisted image analyser (Luzex FS; Nikon, Tokyo, Japan) to calculate the densities of small and large myelinated fibres as described previously.[32–34] A fraction of the glutaraldehyde fixed sample was processed for a teased fibre study, in which at least 100 single fibres were isolated; their pathologic condition was assessed microscopically according to criteria described previously.[32 35] The second portion of the specimen was fixed in 10% formalin solution and embedded in paraffin. Sections were cut by routine methods and stained with haematoxylin and eosin as well as by the Klüver-Barrera and Masson trichrome methods. Control values were obtained from 13 autopsy cases in which patients died of non-neurologic diseases (48.5 (SD 23.5) years of age; male:female, 7:6). Specimens were processed in the same manner as for HNPP patients.

Statistical analysis

Quantitative data are presented as the mean (SD) and were compared with control values using the Mann-Whitney U test. To determine the relationship of electrophysiological and histopathological indices and age at examination, Pearson's correlation coefficient analysis was carried out. To determine whether worsening of these indices in HNPP patients with aging was significantly greater than in normal controls, regression slopes of patient and control groups were compared. Values of p less than 0.05 were considered to indicate significance.

RESULTS

Clinical features

The age at first awareness of neuropathic symptoms in the 48 probands was 33.1 (SD 19.3) years (table 1). The male:female ratio was 38:10. An obvious family history of recurrent transient nerve palsies was present for 24 patients (50%). Only one patient (2%) reported athletic impairment during childhood. Deformity in the distal part of the lower limbs such as hammer toe or pes cavus was present in two patients (4%). Atrophy was noted in the leg in six patients (13%). The pattern of neuropathic symptoms was multiple mononeuropathy associated with recurrent transient nerve palsies in 41 patients (85%), while the other seven (15%) manifested mainly a symmetric polyneuropathy pattern. A history of transient nerve palsy was noted in the median, ulnar, radial, and peroneal nerves in 11 (23%), 18 (38%), seven (15%), and 29 (60%) patients, respectively. Signs of brachial plexus palsy were reported in 10 (21%). With respect to the activities of daily living, all patients were non-disabled or only mildly disabled, except for two (4%) who became unable to walk.

Electrophysiological features

Motor conduction studies showed variable degrees of abnormality in individual nerves (table 2). For the median nerve, MCV was significantly slowed compared to normal controls ($p<0.0001$). This slowing of MCV was present regardless of age at examination, and there was no

significant difference in regression slopes in the correlation between MCV and age at examination (regression slope −0.073 for HNPP *v* −0.064 for controls). DL was very prolonged (179% of controls) and prolongation tended to worsen as age at examination increased (r = 0.47). The CMAP was reduced to various degrees in most patients and showed further reduction with advancing age (r = −0.67; fig 1). Worsening of both DL and CMAP with age was significantly more prominent than in controls, as evident from comparison of regression slopes ($p<0.0001$ and <0.01, respectively).

For the ulnar nerve, mild to moderate slowing of MCV and prolongation of DL were noted regardless of age at examination, while CMAP decreased with advancing age (r = −0.65). CMAP diminution with aging was significantly worse in patients than in controls (regression slope −0.109 for HNPP *v* −0.021 for controls; $p<0.0001$). For the tibial nerve, slowing of MCV and prolongation of DL also were mild to moderate in most patients of all ages. Reduction of CMAP was also present in all ages examined but, in contrast to other nerves, the relationship of reduction to aging was indistinguishable from that in controls (regression slope −0.062 for HNPP *v* −0.069 for controls). For the peroneal nerve, the age associated decrement in CMAP was significantly greater than in controls ($p<0.05$). Slowing of MCV and prolongation of DL were present in patients of all ages, but no significant worsening with aging was seen in comparison with controls.

As for sensory conduction studies, slowing of conduction velocity was present as in motor nerves. SCV of the median nerve tended to slow with increasing age at examination (r = −0.41). This age associated worsening was significantly greater than in controls ($p<0.05$), while SCV of the ulnar and sural nerves did not show a correlation with age. Reduction of SNAP was conspicuous in the median (24% of control amplitude), ulnar (28%), and sural (42%) nerves. Age associated reduction of SNAP was seen in the median (r = −0.50), ulnar (r = −0.45), and sural (r = −0.37) nerves, but the rate of change was not worse than in controls.

Duration of CMAP and SNAP was prolonged in all nerves examined compared to normal controls, suggesting the presence of temporal dispersion.[27] Compared to controls, significant age associated worsening was seen only in the SNAP of the median nerve ($p<0.0001$).

Histopathological features

Average total myelinated fibre density in patients' sural nerves was mildly, but not significantly, reduced compared to normal controls (7738 (SD 1253) *v* 8561 (SD 1289) fibers/mm^2; table 3). The density of large myelinated fibres was significantly reduced from that in controls (2458 (SD 730) *v* 3258 (SD 736) fibers/mm^2; $p<0.01$) but that of small myelinated fibres was not (5280 (SD 1025) *v* 5302 (SD 655) fibers/mm^2). Axonal sprouting was not conspicuous in any case. Although the density of large myelinated fibres decreased as age at examination increased (r = −0.70), the rate of reduction was indistinguishable from that in controls (regression slope −27.1 for HNPP *v* −26.0 for controls) because large myelinated fibres were reduced even at younger ages. Teased fibre preparations revealed frequent tomacular change (41.5% (SD 15.8%)). The frequency of segmental

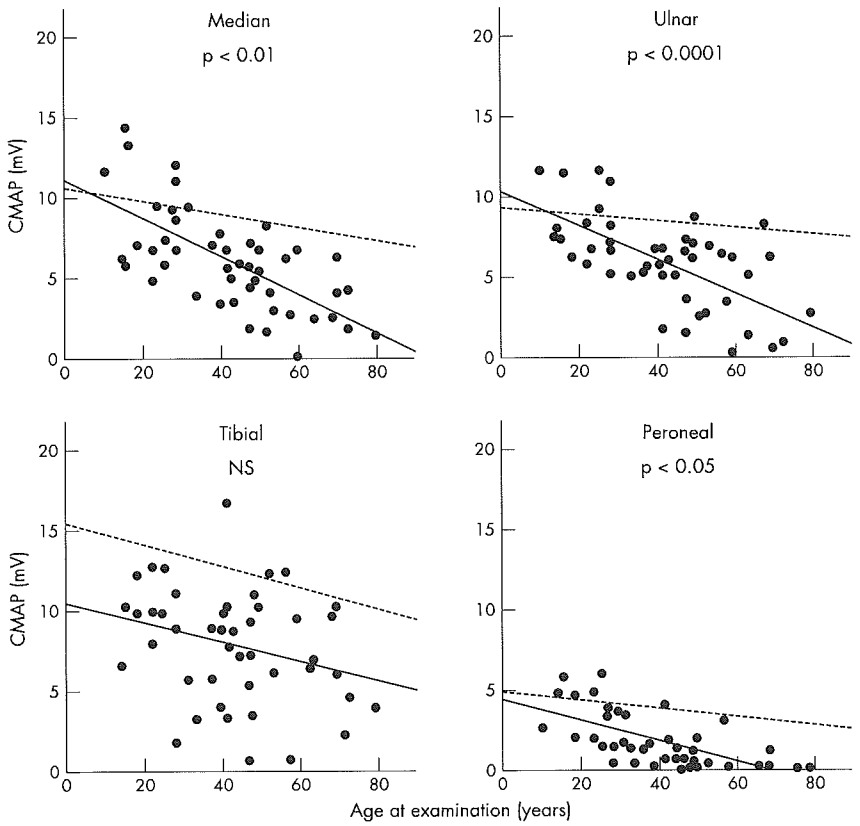

Figure 1 Correlation between CMAP and age at examination in HNPP patients and normal controls. Filled circles represent indices in HNPP patients, bold lines represent regression lines for HNPP patients, and broken lines represent regression lines for normal controls. Comparing regression slopes of normal controls and HNPP patients, CMAP of the median, ulnar, and peroneal nerves, but not the tibial nerve, in HNPP patients were significantly more reduced with increasing age at examination.

Table 2 Nerve conduction studies

	HNPP							Controls		
	Nerve conduction measures				Correlation to aging				Correlation to aging	
	n	Mean (SD)	% of controls	p Values for controls*	r †	Regression slope	p Values for controls‡	Mean (SD)	r †	Regression slope
Motor conduction										
Median nerve										
MCV (m/s)	47	46.0 (5.3)	80	<0.0001	−0.25	−0.073	NS	57.6 (3.8)	−0.27	−0.064
DL (ms)	47	6.1 (1.8)	179	<0.0001	0.47	0.046	<0.0001	3.4 (0.4)	0.19	0.005
CMAP (mV)	48	6.3 (3.2)	77	<0.0001	−0.67	−0.122	<0.01	8.2 (2.9)	−0.24	−0.042
Duration (ms)	32	5.4 (0.8)	115	<0.001	0.13	0.006	NS	4.7 (0.9)	−0.07	−0.004
Ulnar nerve										
MCV (m/s)	47	46.9 (8.3)	81	<0.0001	0.04	0.018	NS	58.0 (4.6)	−0.22	−0.062
DL (ms)	47	3.8 (0.8)	146	<0.0001	0.17	0.009	NS	2.6 (0.3)	0.06	0.001
CMAP (mV)	48	6.0 (3.0)	81	<0.001	−0.65	−0.109	<0.0001	7.4 (1.8)	−0.20	−0.021
Duration (ms)	28	5.9 (1.2)	116	<0.0001	−0.22	−0.016	NS	5.1 (0.7)	−0.01	−0.001
Tibial nerve										
MCV (m/s)	45	39.6 (4.5)	86	<0.0001	−0.02	−0.006	NS	46.0 (3.8)	−0.34	−0.079
DL (ms)	45	5.5 (1.3)	138	<0.0001	0.15	0.011	NS	4.0 (0.6)	0.11	0.004
CMAPs (mV)	45	7.9 (3.7)	67	<0.0001	−0.29	−0.062	NS	11.8 (3.5)	−0.33	−0.069
Duration (ms)	25	5.7 (1.3)	114	<0.01	−0.18	−0.012	NS	5.0 (0.7)	−0.17	−0.008
Peroneal nerve										
MCV (m/s)	38	35.7 (5.7)	76	<0.0001	−0.11	−0.042	NS	47.4 (4.5)	−0.38	−0.101
DL (ms)	38	7.7 (2.3)	167	<0.0001	−0.002	−0.00004	NS	4.6 (1.1)	0.04	0.002
CMAP (mV)	41	1.9 (1.8)	56	<0.0001	−0.65	−0.067	<0.05	3.4 (2.0)	−0.22	−0.027
Duration (ms)	16	6.4 (0.9)	131	<0.0001	−0.09	−0.006	NS	4.9 (0.9)	−0.17	−0.009
Sensory conduction										
Median nerve										
SCV (m/s)	42	38.6 (10.1)	69	<0.0001	−0.41	−0.235	<0.05	56.3 (5.3)	−0.26	−0.085
SNAP (μV)	48	6.8 (6.2)	24	<0.0001	−0.50	−0.178	NS	28.0 (11.5)	−0.45	−0.327
Duration (ms)	26	0.9 (0.4)	150	<0.0001	0.56	0.011	<0.0001	0.6 (0.1)	−0.11	−0.001
Ulnar nerve										
SCV (m/s)	41	36.8 (8.4)	68	<0.0001	−0.13	−0.069	NS	54.5 (5.5)	−0.28	−0.093
SNAP (μV)	48	6.6 (6.4)	28	<0.0001	−0.45	−0.170	NS	23.8 (10.3)	−0.37	−0.240
Duration (ms)	26	0.9 (0.2)	150	<0.0001	0.08	0.001	NS	0.6 (0.1)	−0.05	−0.00004
Sural nerve										
SCV (m/s)	43	36.4 (6.9)	74	<0.0001	−0.13	−0.052	NS	49.2 (4.8)	−0.12	−0.035
SNAP (μV)	48	7.1 (5.9)	42	<0.0001	−0.37	−0.124	NS	16.8 (7.8)	−0.38	−0.177
Duration (ms)	21	0.9 (0.3)	129	<0.05	0.23	0.004	NS	0.7 (0.1)	0.21	0.002

*Mann-Whitney U test; †Pearson's correlation coefficient; ‡regression slopes of HNPP and controls were compared.
Control values were obtained in 171 normal volunteers for the median nerve, 170 for the ulnar nerve, 161 for the tibial nerve, 171 for the peroneal nerve, and 163 for the sural nerve.
CMAP, compound muscle action potential; DL, distal latency; Duration, duration from the onset to the first crossing of the baseline in the CMAP and duration from the onset of the SNAP to the first negative peak; MCV, motor nerve conduction velocity; NS, not significant; SCV, sensory nerve conduction velocity; SNAP, sensory nerve action potential.

de/re-myelination also was significantly high (25.6% (SD 13.9%), p<0.001). Axonal degeneration was slightly increased (3.6% (SD 3.8%)) and was seen even in young patients in contrast to controls.

DISCUSSION

This study demonstrated clinical, electrophysiological, and histopathological features of Japanese HNPP patients with the 17p11.2 deletion. Although recurrent transient nerve palsies are the characteristic feature of this disease, a minority of patients showed a symmetric polyneuropathy pattern, as previously reported.[16–18 36] Electrophysiological features of slowing of conduction velocities and varying degrees of abnormality among individual nerves, agreed well with previous reports of Western populations.[16–20] Slowing of MCV in our series seemed more marked than in previous reports.[16–18 20] The fact that we only examined probands of HNPP families and did not include affected siblings could

Table 3 Histopathological study of the sural nerve

	HNPP (n = 14)					Controls (n = 13)		
			Correlation to aging				Correlation to aging	
	Mean (SD)	p Values for controls*	r †	Regression slope	p Values for controls‡	Mean (SD)	r †	Regression slope
Myelinated fibre density (no./mm^2)								
Total	7738 (1253)	NS	−0.45	−29.6	NS	8561 (1289)	−0.73	−39.9
Large	2458 (730)	<0.01	−0.70	−27.1	NS	3258 (736)	−0.83	−26.0
Small	5280 (1025)	NS	−0.05	−2.5	NS	5302 (655)	−0.50	−13.9
Teased fibre study (%)								
Tomacular change	41.5 (15.8)	–	−0.21	−0.18	–	–	–	–
Segmental de/re-myelination	25.6 (13.9)	<0.001	0.39	0.30	NS	6.9 (6.5)	0.82	0.22
Axonal degeneration	3.6 (3.8)	NS	−0.35	−0.07	<0.05	1.6 (1.8)	0.81	0.06

*Mann-Whitney U test; †Pearson's correlation coefficient; ‡regression slopes of HNPP and controls were compared.
NS, not significant.

account for the difference, or greater slowing might be characteristic of Japanese patients. In the peroneal nerve, it seems that the amplitude of CMAP is lower and the distribution of DL is wider than in Western populations even in normal controls.[26] Japanese people usually sit on the floor at home, rather than on chairs, and sometimes sit with their legs folded underneath them. This traditional Japanese sitting position may induce peroneal nerve injury.

A striking finding in our study was a reduction in CMAP with increasing age at examination. This feature was observed in the median, ulnar, and peroneal nerves but not in the tibial nerve. The median nerve passes through the carpal tunnel, predisposing it to entrapment injury, while the ulnar and peroneal nerves are vulnerable to repetitive compression injury at the cubital tunnel and fibular head, respectively, as suggested by the high frequency of episodic palsy of these nerves compared with the tibial nerve. Repetitive movement and nerve stretching at these sites also may contribute to injury. Thus, individual nerve-specific CMAP reduction with increasing age probably resulted from the cumulative effects of repetitive damage; conduction slowing caused by demyelination would be prominent at entrapment sites, as previously reported.[16–18 20] In the present study, demyelination also showed progression over time as demonstrated by age associated prolongation of DL and SCV in the median nerve for conduction through the entrapment site. However, in the ulnar and peroneal nerves, where electrophysiological indices were recorded distally from sites vulnerable to compression, no age associated worsening of MCV, SCV, or DL was observed, suggesting that myelin abnormality distal to the entrapment site does not worsen with advancing age. Thus, CMAP reduction in the median, ulnar, and peroneal nerves would reflect secondary axonal involvement complicating demyelination at the entrapment site. This age associated axonal involvement in a primarily demyelinating condition is similar to that observed in CMT1A with PMP22 duplication.[12 14 15] However, unlike CMT1A, axonal damage may not occur unless the nerves are subjected to compression. PMP22 duplication in Schwann cells results in disturbance of axonal cytoskeletal organisation, resulting in distal axonal degeneration and fibre loss.[13] However, the effect of PMP22 deletion on the axonal cytoskeleton is less severe.[13] PMP22 deletion in itself may not cause progressive axonal involvement associated with aging, though compression induced demyelination may elicit secondary axonal loss because of deficient Schwann cell signalling to the axonal cytoskeleton.[37]

SNAP of the median, ulnar, and sural nerves showed marked reduction even in nerves relatively free from compression and tended to decrease with increasing age at examination. Unlike findings for CMAP, however, rates of reduction with aging did not differ significantly from those in normal controls. Sensory axons may be less susceptible than motor nerves to changes caused by entrapment.

Reduction in CMAP and SNAP may be at least partly attributed to dispersion with phase cancellation as a result of demyelinating change, as suggested by significant prolongation of waveform duration.[27 38] Sural nerve biopsy specimens showed a reduction in large myelinated fibre density irrespective of age, which may indicate a developmental abnormality of axons or a loss of axons relatively early in life. This axonal loss also may contribute to reduction in amplitudes. At any rate, reduction in myelinated fibres of sensory nerves in HNPP patients did not appear to be associated with acquired damage at the entrapment sites. Thus, the electrophysiological features of HNPP are a mixture of abnormalities occurring from an early stage in life and acquired features caused by repetitive insults at entrapment sites. One therapeutic strategy in HNPP patients may be directed toward prevention of axonal damage associated with entrapment.

Authors' affiliations
H Koike, M Hirayama, M Yamamoto, H Ito, N Hattori, G Sobue, Department of Neurology, Nagoya University Graduate School of Medicine, Nagoya, Japan
F Umehara, K Arimura, Department of Neurology and Geriatrics, Kagoshima University Graduate School of Medicine and Dental Sciences, Kagoshima, Japan
S Ikeda, Third Department of Medicine, Shinshu University School of Medicine, Matsumoto, Japan
Y Ando, Department of Laboratory Medicine, Kumamoto University School of Medicine, Kumamoto, Japan
M Nakazato, Third Department of Internal Medicine, Miyazaki Medical College, Miyazaki, Japan
R Kaji, Department of Clinical Neuroscience, University of Tokushima, Tokushima, Japan
K Hayasaka, Department of Pediatrics, Yamagata University School of Medicine, Yamagata, Japan
M Nakagawa, Department of Neurology, Kyoto Prefectural University of Medicine, Kyoto, Japan
S Sakoda, Department of Neurology, Osaka University Graduate School of Medicine, Suita, Japan
K Matsumura, Department of Neurology, Teikyo University School of Medicine, Tokyo, Japan
O Onodera, Department of Neurology, Niigata University School of Medicine, Niigata, Japan
M Baba, Department of Neurology, Hirosaki University School of Medicine, Hirosaki, Japan
H Yasuda, Department of Medicine, Shiga University of Medical Science, Otsu, Japan
T Saito, Department of Rehabilitation, Kitasato University School of Allied Health Sciences, Sagamihara, Japan
J Kira, Department of Neurology, Kyushu University Graduate School of Medicine, Fukuoka, Japan
K Nakashima, Department of Neurology, Tottori University School of Medicine, Yonago, Japan
N Oka, Department of Rehabilitation, National Minami-Kyoto Hospital, Joyo, Japan

This work was supported by grants from the Ministry of Health, Labor, and Welfare of Japan.

Competing interests: none declared

REFERENCES

1 **Davies DM.** Recurrent peripheral nerve palsies in a family. *Lancet* 1954;**267**:266–8.
2 **Earl CJ,** Fullerton PM, Wakefield GS, *et al.* Hereditary neuropathy with liability to pressure palsies: a clinical and electrophysiological study of four families. *Q J Med* 1964;**33**:481–98.
3 **Behse F,** Buchthal F, Carlsen F, *et al.* Hereditary neuropathy with liability to pressure palsies. Electrophysiological and histopathological aspects. *Brain* 1972;**95**:777–94.
4 **Madrid R,** Bradley WG. The pathology of neuropathies with focal thickening of the myelin sheath (tomaculous neuropathy): studies on the formation of the abnormal myelin sheath. *J Neurol Sci* 1975;**25**:415–48.
5 **Oda K,** Miura H, Shibasaki H, *et al.* Hereditary pressure-sensitive neuropathy: demonstration of "tomacula" in motor nerve fibers. *J Neurol Sci* 1990;**98**:139–48.
6 **Sander S,** Ouvrier RA, McLeod JG, *et al.* Clinical syndromes associated with tomacula or myelin swellings in sural nerve biopsies. *J Neurol Neurosurg Psychiatry* 2000;**68**:483–8.
7 **Chance PF,** Alderson MK, Leppig KA, *et al.* DNA deletion associated with hereditary neuropathy with liability to pressure palsies. *Cell* 1993;**72**:143–51.
8 **Mariman EC,** Gabreëls-Festen AA, van Beersum SE, *et al.* Prevalence of the 1.5-Mb 17p deletion in families with hereditary neuropathy with liability to pressure palsies. *Ann Neurol* 1994;**36**:650–5.
9 **Tyson J,** Malcolm S, Thomas PK, *et al.* Deletion of chromosome 17p11.2 in multifocal neuropathies. *Ann Neurol* 1996;**39**:180–6.
10 **Lupski JR,** de Oca-Luna RM, Slaugenhaupt S, *et al.* DNA duplication associated with Charcot-Marie-Tooth disease type 1A. *Cell* 1991;**66**:219–32.
11 **Sancho S,** Young P, Suter U. Regulation of Schwann cell proliferation and apotosis in PMP-deficient mice and mouse models of Charcot-Marie-Tooth disease type 1A. *Brain* 2001;**124**:2177–87.
12 **Dyck PJ,** Karnes JL, Lambert EH. Longitudinal study of neuropathic deficits and nerve conduction abnormalities in hereditary motor and sensory neuropathy type 1. *Neurology* 1989;**39**:1302–8.
13 **Sahenk Z,** Chen L, Mendell JR. Effects of PMP22 duplication and deletions on the axonal cytoskeleton. *Ann Neurol* 1999;**45**:16–24.

14 **Krajewski KM**, Lewis RA, Fuerst DR, *et al.* Neurological dysfunction and axonal degeneration in Charcot-Marie-Tooth disease type 1A. *Brain* 2000;**123**:1516–27.
15 **Hattori N**, Yamamoto M, Yoshihara T, *et al.* Demyelinating and axonal features of Charcot-Marie-Tooth disease with mutations of myelin-related proteins (PMP22, MPZ and Cx32): a clinicopathological study of 205 Japanese patients. *Brain* 2003;**126**:134–51.
16 **Gouider R**, LeGuern E, Gugenheim M, *et al.* Clinical, electrophysiologic, and molecular correlations in 13 families with hereditary neuropathy with liability to pressure palsies and a chromosome 17p11.2 deletion. *Neurology* 1995;**45**:2018–23.
17 **Pareyson D**, Scaioli V, Taroni F, *et al.* Phenotypic heterogeneity in hereditary neuropathy with liability to pressure palsies associated with chromosome 17p11.2–12 deletion. *Neurology* 1996;**46**:1133–7.
18 **Mouton P**, Tardieu S, Gouider R, *et al.* Spectrum of clinical and electrophysiologic features in HNPP patients with the 17p11.2 deletion. *Neurology* 1999;**52**:1440–6.
19 **Andersson P-B**, Yuen E, Parko K, *et al.* Electrodiagnostic features of hereditary neuropathy with liability to pressure palsies. *Neurology* 2000;**54**:40–4.
20 **Li J**, Krajewski K, Shy ME, *et al.* Hereditary neuropathy with liability to pressure palsy: the electrophysiology fits the name. *Neurology* 2002;**58**:1769–73.
21 **Koike H**, Misu K, Ikeda S, *et al.* Type I (transthyretin Met30) familial amyloid polyneuropathy in Japan: early- vs late-onset form. *Arch Neurol* 2002;**59**:1771–6.
22 **Yamamoto M**, Yasuda T, Hayasaka K, *et al.* Locations of crossover breakpoints within the CMT1A-REP repeat in Japanese patients with CMT1A and HNPP. *Hum Genet* 1997;**99**:151–4.
23 **Kiyosawa H**, Lensch MW, Chance PF. Analysis of the CMT1A-REP repeat: mapping crossover breakpoints in CMT1A and HNPP. *Hum Mol Genet* 1995;**4**:2327–34.
24 **Yamamoto M**, Keller MP, Yasuda T, *et al.* Clustering of CMT1A duplication breakpoints in a 700 bp interval of the CMT1A-REP repeat. *Hum Mutat* 1998;**11**:109–13.
25 **Kimura J**. Principles and variations of nerve conduction studies. In: Kimura J, ed. *Electrodiagnosis in disease of nerve and muscle: principles and practice*, 3rd ed. New York: Oxford University Press, 2001:91–129.
26 **Kimura J**. Assessment of individual nerves. In: Kimura J, ed. *Electrodiagnosis in disease of nerve and muscle: principles and practice*, 3rd ed. New York: Oxford University Press, 2001:130–77.
27 **Kimura J**, Machida M, Ishida T, *et al.* Relation between size of compound sensory or muscle action potentials, and length of nerve segment. *Neurology* 1986;**36**:647–52.
28 **Gilliatt RW**, Melville ID, Velate AS, *et al.* A study of normal nerve action potentials using an averaging technique (barrier grid storage tube). *J Neurol Neurosurg Psychiatry* 1965;**28**:191–200.
29 **Kimura J**. The carpal tunnel syndrome: localization of conduction abnormalities within the distal segment of the median nerve. *Brain* 1979;**102**:619–35.
30 **Sobue G**, Yasuda T, Mitsuma T, *et al.* Expression of nerve growth factor receptor in human peripheral neuropathies. *Ann Neurol* 1988;**24**:64–72.
31 **Misu K**, Hattori N, Nagamatsu M, *et al.* Late-onset familial amyloid polyneuropathy type I (transthyretin Met 30-associated familial amyloid polyneuropathy) unrelated to endemic focus in Japan: clinicopathological and genetic features. *Brain* 1999;**122**:1951–62.
32 **Sobue G**, Hashizume Y, Mukai E, *et al.* X-linked recessive bulbospinal neuronopathy, a clinicopathological study. *Brain* 1989;**112**:209–32.
33 **Hattori N**, Ichimura M, Nagamatsu M, *et al.* Clinicopathological features of Churg-Strauss syndrome-associated neuropathy. *Brain* 1999;**122**:427–39.
34 **Koike H**, Iijima M, Sugiura M, *et al.* Alcoholic neuropathy is clinicopathologically distinct from thiamine-deficiency neuropathy. *Ann Neurol* 2003;**54**:19–29.
35 **Dyck PJ**, Giannini C, Lais A. Pathologic alterations of nerves. In: Dyck PJ, Thomas PK, Griffin JW, *et al*, eds. *Peripheral neuropathy*, 3rd ed. Philadelphia, PA: WB Saunders, 1993:514–95.
36 **Korn-Lubetzki I**, Argov Z, Raas-Rothschild A, *et al.* Family with inflammatory demyelinating polyneuropathy and the HNPP 17p12 deletion. *Am J Med Genet* 2002;**113**:275–8.
37 **de Waegh SM**, Lee VM, Brady ST. Local modulation of neurofilament phosphorylation, axonal caliber, and slow axonal transport by myelinating Schwann cells. *Cell* 1992;**68**:451–63.
38 **Rhee E**, England J, Summer AJ. A computer simulation of conduction block: effects produced by actual block versus interphase cancellation. *Ann Neurol* 1990;**28**:146–56.

PAPER

Progression and prognosis in pure autonomic failure (PAF): comparison with multiple system atrophy

N Mabuchi, M Hirayama, Y Koike, H Watanabe, H Ito, R Kobayashi, K Hamada, G Sobue

J Neurol Neurosurg Psychiatry 2005;**76**:947–952. doi: 10.1136/jnnp.2004.049023

See end of article for authors' affiliations

Correspondence to: Dr Gen Sobue, Department of Neurology, Nagoya University Graduate School of Medicine, Nagoya 466–8550, Japan; sobueg@med.nagoya-u.ac.jp

Received 6 July 2004
In revised form 15 October 2004
Accepted 15 October 2004

Objective: To clarify the progression of autonomic symptoms and functional deterioration in pure autonomic failure (PAF), particularly in comparison with multiple system atrophy (MSA).
Methods: The investigation involved eight patients with PAF (M/F = 7/1; mean age at onset, 57 years) and 22 with probable MSA matched for age at onset (M/F = 14/8; onset 56 years). Subjects were followed up for neurological symptoms, activities of daily living, and autonomic function for more than seven years. Autonomic functional tests were carried out.
Results: In PAF, fainting or sudomotor dysfunction occurred first, followed by constipation and syncope. Urinary dysfunction developed late, and respiratory dysfunction was not evident. This clinical course contrasted sharply with that in MSA, where early urinary dysfunction usually proceeded to sudomotor dysfunction or orthostatic hypotension ($p = 0.004$), followed by respiratory dysfunction ($p = 0.0004$). Results of pharmacological tests also distinguished PAF from MSA. Progression and prognosis in patients with PAF did not worsen, unlike the steady progressive autonomic dysfunction in MSA ($p<0.0001$, $p<0.0001$, $p = 0.0009$, and $p = 0.003$, for progression to modified Rankin scale grade III, IV, V, and death, respectively).
Conclusions: The time course and pattern of progression of autonomic failure differed significantly between PAF and MSA. Patients with PAF had slower functional deterioration and a better prognosis.

Pure autonomic failure (PAF) is a sporadic idiopathic neurodegenerative disorder characterised by gradually progressive severe autonomic disturbances without other neurological features. In the past, PAF was defined as severe orthostatic hypotension without other neurological deficits, and was referred to as idiopathic orthostatic hypotension. However, this has proved to be a heterogeneous condition, including diseases such as PAF, acute autonomic neuropathy, the early stages of Shy–Drager syndrome, and Parkinson's disease with autonomic failure.[1–6]

Bannister *et al*[7] classified primary autonomic failure into three categories: Parkinson's disease with autonomic failure, multiple system atrophy (MSA), and pure autonomic failure. In 1996, a consensus statement was established concerning PAF,[8] but it has remained uncertain whether the autonomic failure of PAF can readily be distinguished from those of MSA and Parkinson's disease with autonomic failure. In addition, although the clinical course of both MSA and Parkinson's disease with autonomic failure has been described to some extent, details of the natural history of PAF have not been fully assessed because of its rarity and very slow progression.[9–11] Previous reports have noted longer survival in patients with PAF than in those with MSA.[3 12–15] Orthostatic hypotension and anhidrosis/hypohidrosis are the main clinical symptoms in PAF, but their severity, prognosis, and progression have been only incompletely assessed. To clarify the clinical features, particularly the natural course of PAF, we observed eight patients who fulfilled the PAF consensus statement and maintained a follow up for at least five years. We show that their features are distinct from those of another form of primary autonomic failure, MSA.

METHODS

Patients

We examined eight patients with PAF (seven men, one woman; mean (SD) age at onset, 57 (14) years; mean age at first evaluation, 68 (12) years; mean duration from onset to most recent evaluation, 19 (10) years) who were referred to the Nagoya University Hospital or its affiliated hospitals in Aichi prefecture between 1988 and 1997. We evaluated these patients clinically from onset for between seven and 32 years. We reviewed the clinical records preceding our own follow up period, and also obtained information by interviewing the patients and family members.

According to the consensus statement,[8] PAF is characterised by orthostatic hypotension, various other autonomic signs without more widespread neurological involvement, and a low resting supine plasma noradrenaline concentration. The statement acknowledged that some patients would later prove to have other disorders such as MSA,[8] but did not state how long a period of follow up was required to confirm a diagnosis of PAF. Early MSA with predominant autonomic failure is particularly difficult to distinguish from PAF. We estimated that most MSA patients can be diagnosed by follow up for five years or more after onset,[8 16] and we therefore serially examined putative PAF patients for more than five years from onset to exclude those with MSA. We also excluded patients with acute autonomic neuropathy, Parkinson's disease with autonomic failure, and other diseases presenting with autonomic signs by neurological examination, imaging (magnetic resonance imaging and positron emission tomography), and neurophysiological tests.

We also investigated 22 probable MSA patients[17] matched according to age at onset (14 men, eight women; mean age at onset, 56 (8) years; mean age at first autonomic test, 61 (7) years; mean interval from onset, 8 (3) years) who had detailed clinical information particularly concerning autonomic features, and follow up intervals from over five years to 16 years after onset. All patients with MSA presented with autonomic failure as an initial symptom or with predominant autonomic failure at their first clinical visit, and fulfilled the criteria for a probable MSA diagnosis.[17]

Abbreviations: AVP, arginine-vasopressin; HUT, head up tilt test; MSA, multiple system atrophy; PAF, pure autonomic failure

Table 1 Clinical profiles of eight patients with pure autonomic failure at their first visit

Variable	Patient 1	2	3	4	5	6	7	8
Sex	M	M	M	M	M	M	M	F
Onset age (y)	35	68	72	78	50	52	51	50
Time until first evaluation (y)	17	1	10	5	27	7	5	13
Duration of observation (y)	32	7	12	12	32	14	15	29
Hypohidrosis	+	+	+	+	+	+	+	+
Faintness	+	+	+	+	+	+	+	+
Syncope	−	−	−	−	+	+	+	+
Constipation	+	−	−	−	+	−	+	−
Difficulty in urination	−	−	+	−	+	−	−	−
Incontinence/urinary urgency	−	−	−	−	−	+	+	+
Respiratory disturbance	−	−	−	−	−	−	−	−
Plasma noradrenaline (pg/ml) *	30	43	25	83	50	34	14	10
Orthostatic hypotension	+	+	+	+	+	+	+	+
Denervation supersensitivity	+	+	+	+	+	+	+	+
Modified Rankin scale	0	0	0	0	0	0	0	0

*Normal range 150 to 450 pg/ml.
F, female; M, male; y, years.

Procedures

We evaluated all eight patients with PAF and 22 with MSA with a passive multistage head up tilt test (HUT) and a noradrenaline infusion test. The HUT was performed as follows. Blood pressure and heart rate were measured continuously by tonometry (SA-250; Colin, Komaki, Japan). After blood pressure stabilised at the supine stage, changes in blood pressure and heart rate were recorded continuously through 20°, 40°, and 60° head up tilting for five minutes each. Orthostatic hypotension was defined as a fall in systolic blood pressure of more than 30 mm Hg during the 60° head up tilt.[18]

Blood samples were collected at the rested supine stage and after 60° head up tilting from all patients for evaluation of plasma noradrenaline and arginine-vasopressin (AVP). Differences in AVP between after 60° head up tilting and the supine position were calculated as ΔAVP. Additionally, a noradrenaline infusion test was carried out as follows. A very low (0.3 μg/min) or a low (3 μg/min) concentration of noradrenaline was infused intravenously while blood pressure was monitored for changes. If diastolic or systolic blood pressure rose by more than 10 mm Hg or 25 mm Hg, respectively, the patient was considered to have denervation supersensitivity involving the sympathetic nervous system.[19] Four patients were re-evaluated two, five, six, and 11 years later, respectively. We also carried out ^{123}I-metaiodebenzylguanidine (MIBG) scintigraphy and evaluated the heart/mediastinum (H/M) ratio from delayed images, as previously described.[20–22]

We followed up all eight patients and noted the time points when new autonomic symptoms appeared, including hypohidrosis, faintness and syncope, constipation, urinary dysfunction, impotence, and respiratory distress, and considered such clinical features in sequence to assess the natural clinical course. We evaluated hypohidrosis in terms of inspection of the skin and recording of patient symptoms. Dry skin or reduced perspiration was noted on some parts of the body, with compensatory hyperhidrosis elsewhere. Patients often noted their reduced perspiration in summer and felt severe fatigue, which sometimes limited their capacity for outdoor work. Faintness was defined as a floating sensation while in the upright position without loss of consciousness, or as symptomatic orthostatic hypotension during the head up tilt test. Syncope was defined as a blackout or loss of consciousness, including severe blurred vision. Constipation was defined by the passage of stools at intervals of three days or more, or complaints of straining. Urinary dysfunction was defined as urination twice at night or more than five times in the daytime, urinary urgency, incontinence, or difficulty in urination. Impotence was defined as difficulty in achieving normal sexual function. Respiratory disturbances were defined either as the presence of sleep apnoea, including heavy snoring, or as difficulty in respiration. Onset of an autonomic symptom was defined as the time when the patient first noted the symptom.

Statistics

The Mann–Whitney U test for non-parametric statistics was used as appropriate. Kaplan–Meier analyses were employed to estimate the natural course of autonomic features and disease progression, assessed by the modified Rankin scale in both PAF and MSA patients. Log-rank test statistics were used to determine whether the Kaplan–Meier curves differed between PAF and MSA. Calculations were done using the statistical software package Stat View (Abacus Concepts, Berkeley, California, USA). Statistical significance was defined as a probability (p) value of <0.05.

RESULTS

Clinical profiles of PAF on the first visit to the hospitals

Clinical profiles of the eight patients with PAF at their first examination at our hospital are presented in table 1. They had many complaints suggesting autonomic disturbances, but the specific features varied. The earliest age at onset was 35 years, and the latest was 78 years. The interval from onset to presentation at our hospital varied from one to 27 years. Each patient showed various autonomic disturbances at that time, but faintness and hypohidrosis had been experienced by all patients. Other autonomic symptoms were as follows: urinary dysfunction in five, syncope in four, constipation in three, and impotence in two. All patients had very low plasma noradrenaline concentrations, orthostatic hypotension, and denervation supersensitivity according to the noradrenaline infusion test.

Clinical manifestations of MSA

The initial symptoms in all 22 patients with MSA were those of autonomic failure. Median time from onset to the presence of concomitant autonomic and motor manifestations (evolution from onset to probable MSA) was 2.0 years (range 1 to 10). At the first clinical visit, seven of the 22 patients presented with severe autonomic failure but failed to fulfil consensus diagnostic criteria of MSA.

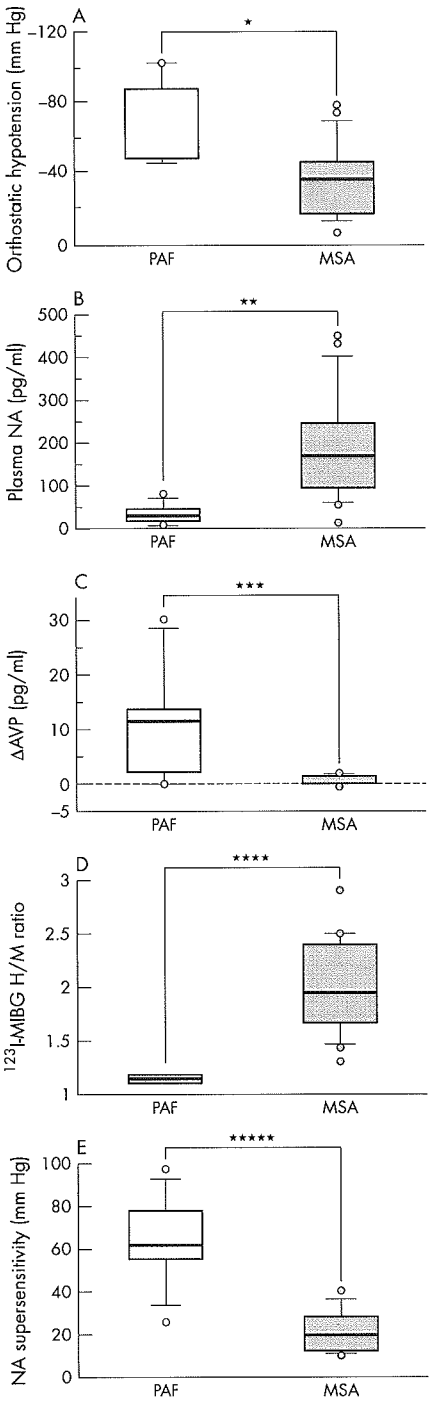

Figure 1 Box and whisker plot of the autonomic nervous testing comparing pure autonomic failure (PAF) with multiple system atrophy (MSA). (A) Systolic blood pressure fall during orthostatic hypotension. (B) Plasma noradrenaline (NA) concentration. (C) Differences in arginine-vasopressin (AVP) concentration between 60° head up tilt and supine posture calculated as ΔAVP. (D) Heart/mediastinum (H/M) ratio from ^{123}I-metaiodobenzylguanidine (MIBG) delayed imaging. (E) Systolic blood pressure increase during noradrenaline infusion test. *p = 0.004, **p = 0.0003, ***p = 0.003, ****p = 0.002, *****p = 0.0004, Mann–Whitney U test.

Autonomic nervous system testing in PAF and MSA

We found significant differences between PAF and MSA patients with respect to the following:

- *orthostatic hypotension* evaluated by the head up tilt test (mean (SD): PAF, 68.9 (22.5) mm Hg; MSA, 36.3 (20.4) mm Hg; p = 0.004 (fig 1A);
- *noradrenaline concentration*: PAF, 36.1 (23.2) pg/ml; MSA, 189.9 (121.9) pg/ml; p = 0.0003 (fig 1B);
- *ΔAVP*: PAF, (10.7) pg/ml; MSA, 0.34 (0.62) pg/ml; p = 0.003 (fig 1C);
- *H/M ratio*: PAF, 1.15 (0.05); MSA, 2.04 (0.44); p = 0.002 (fig 1D);
- *noradrenaline infusion test*: PAF, 70.1 (23.2) mm Hg; MSA, 23.7 (11.0) mm Hg; p = 0.0004 (fig 1E).

Clinical course of autonomic failure

Kaplan–Meier curves depicting the natural clinical course of PAF and MSA are shown in fig 2. Hypohidrosis, faintness and syncope, constipation, urinary dysfunction, and respiratory disturbance were assessed sequentially.

Hypohidrosis

Six patients noted hypohidrosis or anhidrosis as an initial symptom, and seven became aware of hypohidrosis within five years of onset. Hypohidrosis was one of the earliest and most important symptoms of patients with PAF. In contrast, patients with MSA noted hypohidrosis at a significantly later stage of disease (p = 0.027).

Faintness and syncope

These symptoms represented orthostatic hypotension. Usually faintness preceded syncope. Faintness was often noted as an initial autonomic symptom in PAF. Four of eight patients first noted hypohidrosis in the same year as they first experienced faintness. In our series, five patients complained of faintness as an initial symptom, and seven noted faintness within five years of onset. Syncope appeared at (mean (SD)) 6 (7) years after the onset of faintness, and half the patients had experienced syncope within five years. However, two patients first noted syncope more than 19 years after experiencing faintness. In patients with MSA, faintness was observed later in the course of illness, with risk of progression to syncope differing significantly between the two groups (p = 0.002).

Constipation

Constipation was among the early symptoms of PAF. In our series, three patients noted constipation as an initial symptom, and five noted constipation within five years of onset; all patients complained of constipation within 13 years. Constipation was the second earliest symptom in our PAF patients, while patients with MSA also complained of constipation at a relatively early stage of disease. No significant differences were seen between the two groups in time from onset of first symptom to development of constipation (p = 0.46).

Urinary dysfunction

In the early stages few PAF patients noted urinary dysfunction, while at a later stage most patients had this complaint. In our series, urinary dysfunction appeared at (mean (SD)) 9 (9) years after the onset of hypohidrosis, faintness, and constipation. Only three patients noted urinary urgency, urinary frequency, or incontinence in the first five years. Among types of urinary dysfunction, difficulty in urination was rare in PAF patients. We evaluated the results of urodynamic studies in five of the eight PAF patients, at four,